Major transitions in early coral development: novel insights enabled by visualisation of a comprehensive transcriptomic dataset for *Acropora millepora*

Ramona Brunner[1,2*], Mila Grinblat[1,2*], Aurelie Moya[1,2*], Sylvain Foret[3‡], David C Hayward[3], Bruno Lapeyre[1,4], **Eldon E Ball**[3], Ira Cooke[2,5], **David J Miller**[1,2]

[1]ARC Centre of Excellence for Coral Reef Studies, James Cook University, Townsville, QLD 4811 Australia
[2]Molecular Genetics Unit, James Cook University, Townsville, QLD 4811 Australia
[3]Research School of Biology, Australian National University, Acton, ACT 2601 Australia
[4]Laboratoire d'excellence CORAIL, Centre de Recherches Insulaires et Observatoire de l'Environnement (CRIOBE), Moorea, B.P. 1013, Papeete, French Polynesia
[5]Department of Marine Biology and Aquaculture, James Cook University, Townsville, QLD 4811 Australia

[‡]Deceased
Email addresses: RB (ramona.brunner@my.jcu.edu.au), MG (mila.grinblat@my.jcu.edu.au), AM (aurelie.moya@gmail.com), DH (david.hayward@anu.edu.au), BL (viso3841@gmail.com), EB (eldon.ball@anu.edu.au), IC (ira.cooke@jcu.edu.au), DM (david.miller@jcu.edu.au)

Corresponding authors: EB and DM

Keywords: Maternal-zygotic transition, juvenile-adult transition, metamorphosis, coral development, larval settlement

Ethics and integrity statement: Our work does not require ethics approval, but all work involving the biota of the Great Barrier Reef requires approval by The Great Barrier Reef Marine Park Authority (GBRMPA) which rigorously assesses research plans before issuing appropriate permits and carries out routine surveillance. The work described here was conducted under GBRMPA permit G13/36196.1. The authors were all directly involved in the work and all have been consulted on draft and final versions of the manuscript. All analyses have been subject to scrutiny by other authors and can be confirmed using the web-based tool that we have released (see below).

Data availability: The transcriptome data and web-based browser reported here are available at https://amil-deview.mmb.group/. The source code is available at https://github.com/iracooke/amil2_dev.

Funding statement: This work was supported by grant numbers DP170104734, FS110200046 and CE14100020 from the Australian Research Council

The authors declare no conflicts of interest

Ethics approval, patient consent and clinical trial registration are not required for this work

Permission to reproduce material from other sources: Permission has been obtained to reproduce parts of Figure 5 from a previous publication by our group (Hayward et al. 2004). Smaller parts of other figures from our previous publications have been included in other figures, as cited in their captions.

Abstract

Background

Given the ecological importance of reef-building corals (Scleractinia), it is perhaps surprising that the molecular mechanisms underlying many of the morphological and metabolic changes during their development remain unclear. In part, this is due to the lack of a comprehensive transcriptomic dataset for any coral. A second challenge in the analysis of such non-model developmental datasets is that the volume of data often complicates its interpretation.

Results

To overcome these limitations, we profiled gene expression in *Acropora millepora* across 26 life stages from unfertilised eggs to juvenile polyps and developed an interactive online tool based on the R-application Shiny to simultaneously visualise changes in the expression of large numbers of genes. As expected, major transcriptomic changes (transitions) occurred during gastrulation and the acquisition of competence. Surprisingly, however, settlement triggered by using the natural inducer CCA did not immediately lead to major changes in gene expression, but a major transition involving many genes was observed 3 - 6 hours after settlement induction.

Conclusions

We hope that providing access to this extensive developmental transcriptome dataset and software to facilitate its analysis will expedite a better understanding of the changes that occur during coral development. The online tool is available at https://amil-deview.mmb.group.

Background

Broadcast spawning corals, such as *Acropora*, release buoyant eggs and sperm and fertilisation occurs in the water column. The early developmental stages are planktonic, ultimately reaching a motile stage known as a planula larva which becomes “competent” – that is, it becomes capable of settlement and metamorphosis - after a period of development of variable duration (Figure 1). Competence is marked by a change in behaviour, from horizontal swimming to swimming into the substratum and testing it for chemical cues. In nature, the settlement of competent larvae generally involves selection of appropriate sites, based on perception of a range of cues that include small molecules, at least some of which are produced by bacteria associated with substrate biofilms and algae (e.g. Tebben et al. 2015; Siboni et al. 2020; Quinlan et al. 2023; Turnlund et al. 2025). The quality and nature of available light also plays a part in settlement site selection in the case of many reef-building corals (Mason and Cohen, 2012; Strader et al. 2015; Mason et al. 2023).

Various aspects of early coral development have previously been studied (Table 1), with the initial focus being characterisation of individual genes homologous to those playing key developmental roles in bilaterians (Ball et al. 2002; Hayward et al. 2002; Ball et al. 2004; Hayward et al. 2004). The first larger scale analyses were based on microarrays (Grasso et al. 2008; Reyes-Bermudez et al. 2009; Grasso et al. 2011), 454 GSFlx sequencing (Meyer et al. 2009), SOLiD sequencing (Meyer et al. 2011) or subtractive hybridisation (Hayward et al. 2011). More recent studies have used high-throughput DNA sequencing technologies to characterise specific developmental

stages (Summarised in Table 1). Much of this work has focussed on members of the Acroporidae (genera Acropora and Montipora), with sampling regimes designed to address specific questions. For example, Chille et al. (2021) concentrated on gene expression changes *in Montipora digitata* during the maternal/zygotic transition (MZT). However, two recent developmental studies on *M. digitata* have gone beyond transcriptomics and are particularly relevant to the work presented here. He et al. (2024) combined spatial gene expression data with a comprehensive temporal dataset to study the segmentation of the gastric cavity, and Huffmeyer et al. (2025) supplemented transcriptomic data with metabolomic analyses to investigate the nutritional shift from maternal lipids to symbiont photosynthates in this vertically transmitting coral. Much higher cellular resolution expression datasets are becoming available for scleractinians (Levy et al. 2021; Gilbert et al. 2024; Ramon-Mateu et al. 2025), but so far these have been limited to a few developmental stages.

To address the need for a comprehensive transcriptomic dataset, we profiled gene expression of *Acropora millepora* across 26 life stages from fertilised eggs to juvenile polyps and developed an interactive online tool based on the Shiny web framework to visualise changes in the expression of groups of genes. We present an overview of the data, focussing on major transitions in gene expression and on processes not previously investigated, but hope that further exploration of the dataset via the website facilitates progress towards solutions for the crises currently faced by coral reefs worldwide. Our study also reveals the importance of combining spatial expression data, as revealed by in situ hybridisation, with the data obtained by RNAseq, in order to better understand gene function.

130

131 **Materials and Methods**

132

133 Colonies of *Acropora millepora* were collected at Orpheus Island, Queensland,
134 Australia, (18.6141° S, 146.4892° E) under GBRMPA permit G13/36196.1 shortly
135 before they spawned at approximately 9pm on 21 November 2013. The samples
136 sequenced were the result of crosses between two colonies and were raised in three
137 separate flow-through tanks to control for tank effects.

138

139 Material was collected from 26 different time points of which 14 were sampled before
140 and 12 after settlement induction. Pre-settlement, samples were collected from
141 unfertilised eggs, at 5 hours post-fertilisation (hpf; 16-64 cell stages), 13hpf
142 (prawnchip), 18hpf, 23hpf, 29hpf, 35hpf, 40hpf (sphere, some swimming), 45hpf
143 (spheres, all swimming), 57hpf, 69hpf, 81hpf (planulae prior to the searching phase),
144 93hpf (searching planulae) and at 133hpf. At these stages, approx. 500 embryos per
145 replicate (n=3) and cross (n = 2) were immersed in 2 mL ethanol (100%). This
146 caused them to sink to the tube bottom, so that the overlying liquid was removed
147 before tubes were snap-frozen in liquid nitrogen.
148 To assess settlement competency, between 69 and 93hpf, aliquots of planulae were
149 exposed (independently) to either ethanolic extracts of the crustose coralline alga
150 (CCA) *Porolithon onkodes*, (kindly provided by Mikhail V. Matz) or the neuropeptide
151 Hym-248, both of which are known to induce settlement of *Acropora* planulae. At the
152 93 hpf stage 100% of planulae rapidly responded to the CCA extract by undergoing
153 settlement followed by metamorphosis, hence the settlement-induced stages used
154 for RNAseq were derived from planulae exposed to this inducer. Post-settlement

155 samples were collected by stocking 144 petri dishes (2 replicates x 3 larval tanks x 2
156 crosses x 12 time points) with respectively 100 larvae at the age of 133 h. Settlement
157 was induced with ethanolic CCA extract in all petri dishes at the same time. At the
158 respective sampling times of 15 minutes after induction (mpi), 30mpi, 1, 2, 3, 6, 9,
159 12, 18, 24, 48 and 72 hours post induction (hpi), unattached larvae were transferred
160 into tubes, and attached settlers were snap-frozen on petri-dishes using liquid
161 nitrogen after excess seawater was decanted. Sample tubes and petri dishes were
162 taken to James Cook University, (Townsville, Australia) in dry-ice, and stored at -
163 80°C until further processing.
164
165 Frozen samples in the plates were submerged in RNAlater-ICE and allowed to thaw
166 overnight at -20°C. Once thawed, RNAlater-ICE was removed and replaced by 2ml
167 of *mir*Vana™ homogenisation buffer. Polyps were gently scraped off the plate with a
168 sterilized scalpel in the homogenisation buffer and transferred into a 2ml tube for
169 immediate processing.
170 For both pre- and post-settlement samples, total RNA was extracted using
171 the *mir*Vana™ miRNA Isolation Kit (Ambion) according to the manufacturer's
172 instructions. RNA quantity and quality were assessed using a NanoDrop ND-1000
173 spectrometer and denaturing gel electrophoresis using standard methods (Russell &
174 Sambrook 2001) before being shipped on dry-ice to AGRF in Brisbane for Hi-Seq
175 paired-end sequencing.
176
177 RNA sequencing data for all samples was first checked using a Nextflow (Di
178 Tommaso et al. 2017) pipeline https://github.com/marine-omics/moqc. This pipeline
179 includes fastqc (v0.11.5; https://www.bioinformatics.babraham.ac.uk/projects/fastqc/)

180 to check raw read quality, and read-level taxonomic classification via krakenuniq
181 (v1.0.2 ; Breitwieser, Baker and Salzberg, 2018) to determine the dominant symbiont
182 genus and check for bacterial or eukaryotic contaminants. All samples were
183 dominated by reads attributable to the coral host but also contained a small fraction
184 (0.5-2%) from Symbiodiniaceae, of which *Durusdinium* was the dominant genus. No
185 samples were flagged as having low quality base calls, excessive adapter
186 contamination or high levels of potential contaminants (eg bacteria).
187
188 After confirming the overall quality of read data for all samples, reads were trimmed
189 using fastp (Chen, Zhou, Chen and Gu, 2018) to remove adapters and low-quality
190 sequences. Trimmed reads were then aligned to a combined reference database
191 consisting of all *Acropora millepora* transcripts predicted from gene models along
192 with the transcriptome of an unnamed *Durusdinium* species (Shoguchi et al. 2021).
193 Alignment was performed using Bowtie2 (v2.5.0; Langmead and Salzberg, 2012) as
194 part of RSEM (v1.3.3; Li, B., Dewey, C.N., 2011) and used to produce transcript level
195 counts for each sample. All of these steps were run using a Nextflow pipeline
196 https://github.com/marine-omics/morp.
197
198 Transcript counts produced by RSEM were imported into R and processed using the
199 variance stabilising transform function in DESeq2 (vv1.38.3; Love, Huber and
200 Anders, 2014) to produce values on a log2 scale for visualisation.
201
202 Functional annotations for *Acropora millepora* transcripts were obtained using a
203 nextflow pipeline (https://github.com/marine-omics/moat) that is primarily based
204 around identifying homologous proteins in Swissprot (downloaded December 2022)

via blastp and blastx (NCBI Blast+ v 2.13.0). In this process, any protein with an evalue less than 1e-5 is considered a hit and the best hit is used to lookup Gene Ontology ID's and a protein name from the Swissprot database. In addition, transcripts were annotated with conserved domains, gene family membership and an alternative Gene Ontology ID inferred using Interproscan (v5.59-91.0; Jones et al. 2014).

Principal component analysis (PCA) was conducted using the prcomp function of the stats package in R with vst normalised counts.

Weighted gene co-expression network analysis (WGCNA) was conducted with normalised data that were filtered for genes with excessive number of missing values or zero-variance using the goodSamplesGenes function of the WGCNA package (Langfelder & Horvath, 2008). The samples were clustered using the function hclust of the stats package (R Core Team, 2024) to detect outliers. One sample collected 3 hpi was removed from the analysis. To determine groups of genes +(modules) with correlated developmental gene expression profiles, a weighted gene co-expression network was constructed blockwise using the function blockwiseModules with a maximum block size of 18000 genes, a minimal module size of 18 and a mergeCutHeight set to 0.25. A signed, scale-free topological overlap matrix for each block was created by choosing a soft threshold power of 12 and a biweight midcorrelation.

To facilitate reuse and rapid exploration of the *Acropora millepora* developmental transcriptome we created an interactive web application using the shiny framework (https://shiny.posit.co/) . This application is hosted on servers provided by the Australian Research Data Commons Nectar Research Cloud to ensure that it is

scalable and highly available for long-term use. Users can access the web application directly at https://amil-deview.mmb.group/ or obtain its source code and the underlying data from our github repository (https://github.com/iracooke/amil2_dev). The application is designed to facilitate access to developmental expression profiles for individual genes or groups of genes. Users can define genes of interest in two ways by either conducting a BLAST search of a sequence or by directly searching for genes with metadata matching a set of gene identifiers, Pfam domains, GO term IDs or text as part of the protein name. Once a list of genes has been identified, the corresponding normalised gene expression data is rapidly retrieved from an sqlite relational database and used to generate an interactive display. When the number of genes is small (default <10) each gene is displayed using a separate line plot generated by the R package ggplot2 (Wickham, 2016) so that detailed changes in the expression of each gene can be carefully inspected. For larger numbers of genes (default>=10) we assume that the user is more interested in broad patterns among genes and the display changes to an interactive heatmap generated with the R package InteractiveComplexHeatmap (Gu and Hübschmann, 2022). In both cases a list of genes with annotation information is also displayed and users can select rows in this table to adjust which genes are displayed in the main display. Comprehensive data and code exporting functions are also provided so that users can easily export both data and R code to reproduce the plots seen in the app to allow further customisation by the user.

255

256

257 **Results**

258

259 **Major transcriptional transitions visualised using DEView**

260 During the development of *A. millepora*, the period immediately following fertilisation
261 (0 – 5h) was characterised by rapid rounds of cell division (Figure. 1) accompanied
262 by relatively limited changes in gene expression (Figure. 2), implying that this phase
263 is driven largely by maternal mRNAs and proteins. After that time more extensive
264 changes in gene expression occurred resulting in resolvable PCA clusters. After
265 completion of gastrulation at 35hpf, embryos were spherical and became motile at
266 45hpf. Elongation from pear- (57hpf) to spindle-shaped larvae (69hpf) resulted in
267 planulae that were not searching at 81hpf but were probing the environment for
268 appropriate settlement sites at 93hpf, by which time they were competent to settle
269 (Figure. 1). At 133hpf, settlement was induced with ethanolic CCA extract but the
270 133hpf transcriptome data represent the untreated state. Settlement induction
271 caused larvae to further elongate at 15mpi before forming disc-like shapes by
272 contracting along the oral-aboral axis. Most larvae were metamorphosed at 2hpi and
273 by 3hpi 100% of larvae had initiated metamorphosis characterised by a six-fold
274 symmetry around an oral pore in the centre. Whereas transcriptome data for the 0-
275 3hpi stages clustered with those for late planula stages, data for 6 – 72hpi stages
276 formed a discrete and well-resolved cluster (Figure. 2) during which metamorphosing
277 polyps developed a 12-fold symmetry and formed tentacles around the oral opening.
278 The polyp initiates calcification at the former aboral part, which becomes the
279 calicoblastic ectoderm.

Differential gene expression analysis (Figure 3) clearly highlights that, in addition to the expected early (13-29hpf) transcriptional events corresponding to zygotic genome activation, major transitions in gene expression also occurred at 81-93hpf and 3-6hpi. The construction of weighted gene co-expression networks (WGCNA; Langfelder & Horvath (2008), which group modules of genes according to correlation in their expression patterns, also support a 3-transition hypothesis of early coral development (Supplementary Figure 1). Whilst such analyses are informative with respect to the major transitions in development, they are less useful for exploration of the expression patterns of subsets of genes in terms of structure or function according to Pfam or Gene Ontology (GO) IDs. To facilitate these latter kinds of analyses, a software tool based on the Shiny web framework (https://shiny.posit.co/) was developed (https://amil-deview.mmb.group/).

One powerful feature of the new software tool is that it allows the simultaneous visualisation of developmental gene expression patterns from a subset of genes defined by gene identifiers, Pfam domains or GO terms. These subsets can be selected for further analyses and comparison based on morphology, behaviour, or gene expression patterns, such as occur during gastrulation and settlement.

Whilst early zygotic gene expression accompanied gastrulation, the major transition at 81-93hpf is likely to correspond to larval competence which is the preparation for settlement and metamorphosis. Both of these transitions have previously received considerable attention (e.g. Hayward et al. 2011; Grasso et al. 2011; Strader et al. 2018). Metamorphosis was underway by 3hpi and was followed by changes in the

305 expression of large numbers of genes (Figure 2, Figure 3). This post-settlement
306 change in the expression patterns of many coral genes has previously received only
307 limited attention (Ishii et al. 2022) and therefore merited closer examination. In what
308 follows we have proceeded chronologically, with a particular focus on processes and
309 classes of genes not discussed in previous studies.
310

311 **Maternal transcripts and the earliest transcriptional events**

312 As in most animals, early post-fertilisation development in corals consists of rapid
313 cell division during which the maternal cytoplasm is serially subdivided (reviewed in
314 Ball et al. 2021), and the transcripts required to facilitate these events are largely
315 provided maternally. Extensive zygotic gene expression appears to be initiated
316 leading into gastrulation (i.e. around 13h post-fertilisation; Figure 1, Figure 2)
317 corresponding to the “prawn-chip” morphology.
318

319 Rapid rounds of cell division during early development require that replication occurs
320 quickly, generating a need for core histone proteins in large amounts to form the
321 H2A/H2B and H3/H4 dimers that constitute the nucleosomes responsible for
322 packaging the DNA into chromatin. As in *Hydractinia* (*Klyxum*) *echinata* (Ayers et al.
323 2023), histone mRNAs are amongst both the most abundant maternal transcripts
324 and earliest expressed zygotic genes in *Acropora* (Figure 4A). Note, however, that
325 the early zygotic (canonical) histone transcript profile is likely to be dominated by the
326 replication-coupled types.
327 Transcripts encoding the core histones H2B, H3 and H4 are particularly abundant in
328 the *Acropora* maternal mRNA complement (Figure 4A), and the zygotic expression

329 of these histone types began early at the onset of gastrulation with a peak at 13-
330 18hpf for H3, H4 and H2B (XP_044167100.1, XP_044175889.1) (Figure 4A).
331 Curiously, however, canonical H2A mRNA was not maternally provisioned at
332 significant levels, instead, one of two H2A.X homologs (H2A.X2; XP_029204486.1)
333 and, to a lesser extent, H2A.V (H2A.F/Z; XP_029205888.1) transcripts were
334 maternal. Levels of mRNA encoding maternal H2A.X in the unfertilised eggs were
335 very high but fell dramatically after 13hpf as zygotic expression of canonical H2A
336 began (e.g. XP_044167969.1), and H2A.X transcripts were essentially absent by
337 29hpf (Figure 4A).
338
339 Gastrulation is characterised by large scale activation of zygotic genes, requiring
340 extensive chromatin modification. Consistent with this, high levels of mRNAs
341 encoding homologs of the histone acetyltransferase (HAT) KAT6A
342 (XP_029189526.2) and SETD2 (XP_029190384.2) were provided maternally (Figure
343 4B). The latter is the only histone methyltransferase capable of generating the
344 H3K36me3 modification essential for transcriptional activation (Michail et al. 2025).
345 Note that both of these genes were reactivated during the post-settlement transition
346 discussed below.
347
348 **The MZT occurring at gastrulation marks the first major developmental**
349 **transition**
350 To date, the process of gastrulation has been the most extensively studied aspect of
351 developmental gene expression in both corals and *Nematostella* (Technau, 2020). In
352 situ hybridisation analyses have shown that orthologs of several key developmental
353 regulators from bilaterians are temporally and spatially expressed in *A. millepora*

consistent with conservation of function. Examples of these include *snail* (Hayward et al. 2004), *brachyury* (Hayward et al. 2015; Yasuoka et al. 2016), *forkhead* (Hayward et al. 2015) and *dpp/bmp4* (Hayward et al. 2002) (Supplementary Figure 2).

With the sole exception of *Pavona*, all complex corals examined to date go through a "prawn chip" stage of early development that corresponds to the early gastrula (Okubo et al. 2013 and references cited there; Okubo et al. 2016). At this stage, a homolog of *Drosophila snail* (XP_029185944.1) was expressed in the presumptive mesendoderm (Hayward et al. 2004). As *snail*-expressing cells are undergoing an epithelial-mesenchymal transition (EMT), one of several *Acropora* genes related to *Drosophila* aristaless (XP_044163657.1/XP_029193169.1) was expressed throughout the presumptive ectoderm (Figure 5). Hence these two genes effectively demarcate the two primary tissue layers of *Acropora* during gastrulation.

The late planula transition corresponds to the acquisition of larval competence

During the period 81-93hpf, many genes show strong down-regulation, but this is immediately followed by the up-regulation of an even larger number of genes during the 93-133hpf time window (Figure 3).

These timepoints correspond to the acquisition of settlement competence and when *Acropora* larvae are searching for cues that identify appropriate settlement sites (eg. Tebben et al. 2015, Siboni et al. 2020, Quinlan et al. 2023, Turnlund et al. 2025) by swimming along the substratum to periodically sample it with the aboral end.

Settlement involves the aboral larval ectoderm making contact with substratum, which is likely coated with attractive and potentially hostile bacteria, and among the upregulated genes a number encode proteins with known or suspected antimicrobial properties. Among them are for example AmAMP1 (Mason et al. 2021; XP_029188806.1), the MAC-Perforin protein apextrin (Miller et al. 2007; Hayward et al. 2011; XP_044181104.1) and the quorum quenching enzyme AmNtNH1 (Mason et al. 2024; XP_029207486.1). Figure 6 summarises developmental expression data for these three genes.

This study also provides the most direct evidence to date in support of Hadfield's hypothesis (Hadfield, 2000) that coral larvae are primed for settlement and metamorphosis via prior gene expression. Whilst several thousands of genes are up or down regulated during the onset of competency (81- 133hpf), settlement and the initiation of metamorphosis largely happen without changes in gene expression (Figure 3). With the caveat that datasets and technologies were much less sophisticated than those presently available, Grasso et al. (2011) came to the same conclusion for *A millepora* based on microarrays, as did Strader et al. (2018) indirectly by correlating expression data for competent larvae with settlement-induced larvae from Meyer et al. (2011).

The post-settlement gene expression transition resembles an MZT in terms of scale and involvement of some specific components

The scale of the post-settlement transition between 3-6hpi resembles that typical of an MZT. In *Acropora*, we estimate that approximately 20% of mRNAs undergo at least a two-fold change in expression level (i.e. are either up- or down-regulated over

403 the 3-6hpi time window). By comparison, in the zebrafish approximately 25% of
404 maternal transcripts are cleared during the MZT (Mishima and Tomari, 2017) and the
405 corresponding number for *Caenorhabditis* is around 33% (Baugh et al. 2003). Many
406 of the mRNAs up-regulated over the 3-6hpi time window in *Acropora* coded for
407 transcription factors or other regulatory proteins involved in chromatin modifications
408 and mRNA processing.
409
410
411 **Chromatin modification during early development and at the post-settlement**
412 **transcriptional transition**
413 Major changes in gene expression patterns also generally involve chromatin
414 modification events, so histone modification and DNA methylation changes are to be
415 expected. Homologs of a number of key chromatin modifiers are differentially
416 expressed at the 3-6hpi transition.
417
418 In many animals, homologs of TET (ten-eleven translocation) are the primary agents
419 responsible for demethylation of 5-methylcytosine residues (MeCpG) in DNA and are
420 required for gene activation (Mohr et al. 2011; Wu and Zhang 2017; Jessop et al.
421 2018). As well as a transient earlier (5hpf) window of expression leading into the
422 early MZT, the *Acropora TET* homolog (XP_029179484.2) was strongly upregulated
423 at the 6hpi time point (Figure 7A), suggesting a role for the *Acropora* TET homolog in
424 relieving repression by erasing pre-existing MeCpG marks.
425

426 DNA methylation is generally associated with repression of transcription, the
427 enzymes associated with maintenance and *de novo* DNA methylation being the DNA
428 methyltransferases DNMT1 and DNMT3, respectively.
429 In the case of *Acropora*, mRNAs encoding the DNA methylases DNMT1
430 (XP_029197815.2) and DNMT3a (XP_029213858.1) were maternally provided,
431 zygotic expression of DNMT1 being detected between 29hpf and 12hpi, despite
432 having faded by 81hpf. Both DNMTs were upregulated 12 to 18hpi (Figure 7A)
433 expression of DNMT3a appeared to be stronger than that of DNMT1 (Figure.7A)
434

435 **mRNA degradation during major transitions in development**

436 Perhaps the major characteristic of MZTs is the elimination of a subset of maternally
437 provided mRNAs (often a major proportion) to facilitate the transition to the zygotic
438 developmental program. The mRNA elimination process employs a range of
439 mechanisms to destabilise or degrade transcripts, but some conserved players have
440 been identified during major transitions, including homologs of the *Drosophila* genes
441 *Pumilio* (Gerber et al. 2006; Rabani et al. 2017) and *Smaug* (Chen et al. 2014) as
442 well as the *Caenorhabditis* protein TRIM71/LIN41 (Spike et al. 2022).
443

444 Transcripts annotated as *Pumilio* (XP_029180703.2 and XP_029180704.2) were
445 maternally provided but were essentially cleared after 29hpf, whereas a distinct
446 Pumilio homolog (XP_044164192.1) was not represented in the maternal mRNA
447 complement but was expressed from 18hpf (Figure 7B). Each of these Pumilio
448 homologs was up-regulated over the 3-6hpi time window after earlier periods of
449 activity.
450

451 Members of the Smaug/SAMD4 family of proteins are highly conserved (yeast to
452 man) regulators of mRNA stability and transcriptional repressors that act in
453 development by binding to specific RNA sequence motifs. Smaug proteins have
454 been implicated in erasing maternal transcripts during the MZT in the early
455 development of diverse animals (Chen et al. 2014; Chille et al. 2021) implying that
456 the Smaug homolog fulfills a similar function in the early development (around 4hpf)
457 of the coral *Montipora capitata*. Although an early "flutter" of Smaug expression,
458 possibly corresponding to that reported in *Montipora* (Chille et al. 2021), was
459 observed in *Acropora* at 5hpf, Smaug (XP_029197445.1) was predominantly
460 expressed at 15mpi - 6hpi (peak) (Figure 7B). A second transcript annotated as
461 Smaug (XP_044163536.1) was mildly up-regulated at 13-18hpf.
462
463 Members of the TRIM71/LIN41 family of E-3 ubiquitin ligases are highly conserved
464 RNA-binding proteins (Aviv et al. 2003) that facilitate major developmental transitions
465 in *Caenorhabditis* (Spike et al. 2022). At least one member of this gene family
466 (XP_029198843.2/XP_029198844.2) is up-regulated at the 3-6hpi time point during
467 *Acropora* development, suggesting that they may also be involved in protein
468 clearance at the 3-6hpi transition.
469
470 **Small RNA processing pathway components**
471 Small RNAs (miRNAs, siRNAs and piRNAs) have important regulatory functions
472 during the development of many bilaterians (Bartel, 2004) and this is likely to also be
473 the case in *Acropora* given that at least some components of the miRNA processing
474 pathway are known to be differentially expressed during the development of
475 *Nematostella* (Praher et al. 2017). In cnidarians, the biogenesis of miRNAs follows a

476 plant-like pathway (Moran et al. 2017), but homologs of some of the enzymes in the
477 animal miRNA processing system are also present and may also participate in
478 miRNA synthesis.
479 To address the possibility of miRNAs participating in gene regulation during early
480 coral development, the expression of components of both the plant and animal
481 processing pathways was investigated (Figure. 8).
482
483 Some of the small RNA processing pathway components were provided maternally,
484 levels of transcripts annotated as Dicer-like (XP_029197160.2) and the HEN1
485 methyltransferase (HEN1MT; XP_029185006.2) being present at high levels. In
486 cnidarians, HEN1 is responsible for methylation of the 3'-ends of both miRNAs and
487 piRNAs, resulting in their stabilisation. The observed upregulation of HEN1 at 93hpf
488 (Figure. 8) is consistent with a role in metamorphosis of *Acropora* larvae, as in
489 *Nematostella* (Modepalli et al. 2018).
490 The maternal mRNA repertoire also included an Argonaute homolog
491 (XP_044181068.1) and a *Acropora* Piwi-like protein (XP_029187700.2/
492 XP_029187701.2) (Figure. 8) that likely function together in transposon silencing
493 during early development, as in *Nematostella* (Fridrich et al. 2020; Bamberger et al.
494 2022). The high abundance of mRNA encoding a homolog of the Maelstrom protein
495 (XP_044166539.1) also attests to the importance of the piRNA-mediated transposon
496 silencing pathway (Matsumoto et al. 2015; Sato and Siomi, 2015) during the earliest
497 stages of coral development.
498 Although not maternal, other miRNA pathway components were expressed very
499 early in development (Figure 8). Transcripts annotated as DGCR8/Pasha
500 (XP_029194207.2) and SRRT/Serrate (XP_044181962.1) were first detected as the

early embryo was going into gastrulation at about 13hpf. For both of these genes, other transcripts carrying the same annotation appeared to be expressed during different stages of development. In the case of SRRT/Serrate, XP_044181962.1 is expressed in the early gastrula but most heavily after the initiation of metamorphosis (6hpi). A second isoform/splice variant (XP_044181963.1) was most highly expressed very early in the settlement process (15mpi - 2hpi) – i.e. prior to what Ishii et al. (2022) referred to as the “point of no return”.

Similarly, the DGCR8/Pasha paralogs or splice variants XP_029194207.2 and XP_029194208.2 seem to have distinct expression profiles during development (data not shown).

In addition to the maternal Piwi-like mRNA (XP_029187700.2/ XP_029187701.2), a second (non-maternal) Piwi (XP_044168784.1/ XP_044168785.1/ XP_044168786.1) was expressed from the early gastrula stage, peaking in expression as the maternal type was fading.

Discussion

The study of early coral (*A. millepora)* development presented here was based on gene expression profiles obtained for 26 developmental stages spanning the period between unfertilised eggs and 3-day-old primary polyps. Downstream analyses via a DEView app revealed three major transcriptomic transitions - the maternal-zygotic transition, the acquisition of competence by planulae (93-133hpf) and a post-settlement transition (3-6hpi) that has not previously received significant attention. This latter novel transition in gene expression resembled an MZT in terms of scale and the involvement of some key genes. In addition to regulatory genes involved in

526 chromatin modification and RNA processing, we focused here on genes likely to
527 have protective roles, specifically those potentially involved in photoprotection, anti-
528 microbial activity and transposon silencing.
529
530 In many animals, mRNAs encoding canonical histones (including H2A) as well as the
531 corresponding proteins are provided maternally at sufficient levels to support the
532 earliest cell division events. To our knowledge, finding that in *Acropora*, an mRNA
533 encoding one H2A.X variant (H2A.XII) replaced that for canonical H2A in the eggs is
534 novel. H2A.X is a histone variant whose best-defined role is in DNA repair (reviewed
535 in Lorkovic and Berger, 2017; Herchenröther et al. 2023). It is closely related to
536 canonical H2A but distinguished from it by the presence of a characteristic C-
537 terminal sequence extension that includes a serine residue subject to
538 phosphorylation generating the gammaH2A.X form which is required for binding at
539 double-stranded DNA breaks (Osakabe and Molaro, 2023). The enzymes
540 responsible for this phosphorylation of H2A.X are Phosphoinositide-3-Kinase-related
541 protein kinases (PIKKs), and at least one PIKK-related protein kinase
542 (XP_029200091.2) is provided maternally in *Acropora*, though it is unclear whether
543 H2A.X is a substrate for this activity.
544
545 Whilst most coral spawning occurs during the night, the gamete bundles (or eggs)
546 released are buoyant so that the earliest developmental events occur near the
547 water's surface. In the present study, *Acropora* larvae became motile 40-45hpf by
548 which time they would have been exposed to two days of direct sunlight. Early
549 developmental stages of corals therefore face exposure to UV radiation at levels that
550 can cause DNA damage, and H2A.X2 mRNA may be maternally provided at high

levels to facilitate maintenance of DNA integrity through the earliest developmental stages. Chille et al. (2021) noted high representation of GO terms associated with DNA repair in the maternal mRNA complement of *Montipora* but did not identify specific genes/proteins. GFP-related proteins are also thought to be involved in DNA protection in corals (Salih et al. 2000; Palmer et al. 2009; Bou-Abdallah et al. 2006; Clarke et al. 2024) and, consistent with the study of Strader et al. (2018), at least four distinct types are expressed during the larval and early polyp stages. Although mRNAs encoding GFPs did not appear to be maternally provided at significant levels, the pigmentation of the eggs of many coral species is consistent with the idea of maternal provision of photoprotective agents that likely include GFP-related proteins, which are known to be long-lived.

Note that in *Acropora* there is a second H2A.X-like gene (H2A.X1; XP_029200990.1 - annotated as H2A-like) that is expressed only at relatively low levels during early development. This second H2A.X isoform (XP_029200990.1) has an N-terminal tyrosine residue replacing the phenylalanine in XP_029204486.1 and has close homologs in *Hydra* (CDG71330.1; 86.47% protein identity to *Acropora*) and *Hydractinia* (now *Klyxum*; AOF43153.1; 87.02% identity) and, like those, is presumed to be the main isoform expressed during post-larval life. In *Hydractinia* (now *Klyxum*) *echinata*, the H2A.X variant AOF43152.1 is expressed specifically in female germ cells along with canonical histone H2A (Torok et al. 2016) and may be functionally equivalent to the maternally provided *Acropora* H2A.X homolog XP_029204486.1 (protein sequence identity of 68.15%).

Comparisons with published studies of coral development

The most interesting observation made here was the extent and nature of the post-settlement transcriptional transition observed at 3-6hpi. This major change in gene expression is more apparent than in previous studies which either did not include post-settlement stages (Strader et al. 2018; Chille et al. 2021) or sampled sparsely pre-settlement (Huffmeyer et al. 2025) or after settlement induction (Ishii et al. 2022, Meyer et al. 2011) (Table 1). Furthermore, comparisons between the work presented here and previously published papers in this field (Table 1) are complicated due to the diversity of species studied, differing temperatures during development, differing sampling points and differing inducers used to trigger settlement and metamorphosis.

Development has been studied primarily in members of the three coral genera *Acropora, Montipora* and *Porites*. Whilst these are all members of the “superfamily” Complexa, and the first two belong to the same coral family (Acroporidae), both *Montipora* and *Porites* spp. maternally transmit Symbiodiniaceae whereas *Acropora* spp. acquire their symbionts from the environment during early life.

Chille et al. (2021) focussed on MZT and therefore studied gene expression changes during development of *Montipora capitata* from unfertilised egg to planula in addition to adults. Some of their MZT results are consistent with those presented here for *Acropora*, for example the expression of Smaug (Figure 7B) and Brachyury (Supplementary Figure 2) in prawn chip and early gastrula.

However, the rate of development of *M. capitata* observed was apparently slower than that of *Acropora*. *Montipora capitata* reached the late gastrula stage after 1.5

599 days, whereas *Acropora* generally reaches the corresponding stage earlier (around
600 30hpf). This demonstrates the complication of relating developmental stages across
601 datasets where interspecific differences can be compounded by the
602 presence/absence of maternal photosymbionts and different rearing temperatures,
603 as higher temperatures accelerate development. Using GO-term data, Huffmeyer et
604 al. (2025) recognised three distinct (but overlapping) phases of gene expression
605 during the early development of *Montipora*.
606 Since morphology reflects changes in gene expression, we have found that
607 comparisons of gene expression based on morphology are more meaningful than
608 those based on time, even in the single species *A millepora*. The post-settlement
609 transition remained unexplored in the study of Chille et al. (2021) since the focus on
610 MZT did not require the sampling of post-settlement stages. The 3-6hpi gene
611 expression transition observed here may correspond to what Ishii et al. (2022) refer
612 to in their study as “the point of no return” (PNR), a point in post-settlement
613 development after which reversibility by aborting settlement and returning to the
614 motile phase is lost. Whilst the Ishii et al. (2022) paper focussed on gene expression
615 changes between three time points during metamorphosis in *Acropora*, comparison
616 between their results and those presented here is complicated by the differing
617 triggers used to drive the process. For *Acropora* spp., external exposure of
618 competent larvae to the *Hydra* GLWamide (Hym-248), directly triggers
619 metamorphosis, essentially overriding the need for external settlement cues (Iwao et
620 al. 2002; Grasso et al. 2011; Attenborough et al. 2019). Whilst Ishii et al. (2022)
621 induced metamorphosis using Hym-248, the study described here triggered
622 settlement by addition of CCA extract, which induces searching behaviour rather
623 than directly driving metamorphosis (Grasso et al. 2011). Hence it is not possible to

624 directly compare developmental timing between these two studies. The 1hpi and
625 6hpi time points in the Ishii paper are likely to correspond to later time points in the
626 present study, as the duration of the settlement period must be several hours longer
627 when using CCA extract compared to Hym-248. The PNR inferred by Ishii as
628 occurring at 4hpi may correspond to the 3-6h transition identified in the present work
629 but note that rates of larval development can be strongly influenced by temperature.
630 The differences in gene expression between untreated (0 hr) and 1 hour after
631 induction described in the Ishii et al. paper are therefore likely to encompass a
632 number of distinct time points in our study, so subtle transcriptional changes
633 occurring during the searching and very early settlement phases were presumably
634 not noted by Ishii et al. (2022).
635

636 **The post-settlement transition – a cnidarian equivalent of the *Caenorhabditis***
637 **"juvenile to adult" transition?**

638 In *Acropora*, the transition from larvae to recruits at 3-6hpi has several parallels to
639 maternal-zygotic transitions (Vastenhouw et al. 2019) regarding the removal of
640 earlier transcripts and genome activation appropriate for stages following the
641 transition. A precedent for such a later transition is provided by *Caenorhabditis*
642 *elegans*, where it is recognised as the juvenile to adult transition (Spike et al. 2022).
643

644 Above, the involvement of homologs of both *Drosophila* Smaug and Pumilio in the
645 mRNA clearance processes during MZT and the juvenile to adult transition at 3-6hpi
646 were highlighted. In addition, two transcripts with the same sequence
647 (XP_029198843.2 and XP_029198844.2) annotated as a member of the
648 TRIM71/LIN41 family of RNA-binding proteins were upregulated during the 3-6hpi

649 transition. Other members of this protein family have important roles in the regulation
650 of both oocyte to embryo (Spike et al. 2022) and juvenile to adult (Aeschimann et al.
651 2019) developmental transitions in *Caenorhabditis*. As in *Caenorhabditis* (Spike et al.
652 2022), this *Acropora* TRIM71/LIN41-related protein is likely to be involved in
653 regulatory changes at the 3-6hpi transition, and on this basis deserves further
654 exploration.
655
656 In addition, peaks in the expression of the DNA demethylase TET (Figure 7A) and of
657 SETD2 (XP_029190384.2) as well as homologs of the histone acetyltransferases
658 HAC5 (XP_029203404.2), KAT5 (XP_029179982.2) and KAT6A (XP_029189526.2)
659 (Figure 4B) around 3-6hpi imply extensive chromatin modification at that time.
660 Presumably, the corresponding proteins function in facilitating transcription of genes
661 required for early polyp development (e.g. He et al. 2024). Transcription factors (TF)
662 strongly up-regulated at the 3-6hpi time point include genes annotated as homologs
663 of FoxB1 (XP029196672.1) and FoxO (XP_029208531.2), Aristaless
664 (XP_029193170.1), Rax (XP_029193171.1), Meis2 (XP_029187327.1) and Otx
665 (XP_029190339.1), whilst homologs of Emx (XP_029211983.2), Pitx2
666 (XP_029179676.1) and Brn3C (XP_029213135.1) were simultaneously down-
667 regulated.
668
669 **Limitations: Heatmaps are useful but tell only part of the story**
670 A caveat in making inferences from heatmaps across developmental stages, and
671 more generally from whole-larvae overall expression levels, is that important subtle
672 changes may be missed. Particularly with transcription factors or other regulatory
673 molecules, low overall levels of expression may have major effects, especially when

restricted to subsets of cells. Consequently, interpreting developmental gene expression requires not only temporal data, but also spatial information from the application of in situ hybridisation or other techniques. This is clearly illustrated in Supplementary Figure 2, which provides expression data for genes implicated in conserved functions during gastrulation.

Whilst in situ hybridisation data show expression of these four genes in smaller subsets of genes across all developmental stages between gastrulation and metamorphosed recruit, the heatmaps show that the expression maxima occur post-settlement rather than at gastrulation around 13 – 18hpf. Only a weaker peak in expression of Brachyury at 13hpf corresponds to the early gastrulation window of expression visualised via in situ hybridisation (Hayward et al. 2015). Consequently, visualisations of spatial expression via in situ hybridisation are required to study the function of selected genes. For example, whilst gene expression data presented in the heatmap suggested functions post-settlement, ISH visualisations revealed that temporal expression of an *Acropora* arx-related gene (XP_044163657.1/XP_029193169.1) during gastrulation closely complements that of snail (Figure 5). This *Acropora* sequence is referred to here as homeobrain, based on its orthology with *Nematostella* XP_048583705.1 (Mazza et al. 2010). Snail and homeobrain respectively demarcate the early mesendoderm and presumptive ectoderm during gastrulation (Figure 5), but both are also expressed at higher levels after settlement-induction where snail expression reaches its expression peak earlier than in the case of homeobrain. Assuming these two genes fulfill similar function during gastrulation and post-settlement, this suggests that a cell migration such as in an epithelial-mesenchymal transition occurs during the initiation of metamorphosis.

698 The upper limit of expression in a heatmap is determined by the genes included in
699 that map so important changes in gene expression may not be as apparent as if the
700 gene was plotted against itself.
701
702 **Expression of the small RNA processing machinery during early development**
703 Despite deep evolutionary divergence between the sea anemones (Actiniaria) and
704 the coral/corallimorpharian lineage, many of the molecular processes underlying
705 early development in *Acropora* closely parallel those described in *Nematostella*
706 (Hayward et al. 2015), and this appears to extend to the machinery for processing
707 small RNAs (miRNAs and piRNAs). However, some differences were observed in
708 the timing of expression of several of genes implicated in small RNA processing.
709 Whilst mRNAs for Vasa1, Maelstrom and Piwi are provided maternally in *Acropora*
710 and *Nematostella*, Vasa2 (aka Vasa-like or DDX4) is also maternal in the coral
711 whereas the corresponding mRNA was not detected until around gastrulation in
712 *Nematostella* (Praher et al. 2017). Whether Dicer/DCL is maternal is unclear in the
713 case of *Nematostella*, whereas mRNA of the *Acropora* homolog of *Nematostella*
714 Dicer 2 (AGW15596.1), encoding XP_029197160.2, is abundant in *Acropora* eggs.
715 In summary, the preliminary data presented here indicate that all or most of the small
716 RNA processing machinery is either maternal or expressed very early in *Acropora*
717 development. It is therefore likely that, in addition to roles for some of these
718 components in transposon silencing, miRNAs are likely to have important regulatory
719 roles in the early development of *Acropora*.
720
721 **Heatmaps enable identification of candidate genes for key roles in early**
722 **development**

723 A major strength of the DEView app is that it provides a means of scanning classes
724 of genes individually or collectively for their expression patterns across early coral
725 development, allowing identification of candidates for roles in specific processes,
726 including settlement induction and the initiation of calcification. Whilst significant
727 progress has recently been made, we have as yet a relatively limited understanding
728 of the nature and recognition of settlement cues (Hadfield, 2011; Tran and Hadfield,
729 2012; Ball et al. 2021; Turnlund et al. 2025). The larvae of many corals select
730 appropriate settlement sites by detection of small molecules that either favour or
731 discourage settlement (e.g. Morse et al. 1988; Negri et al. 2001; Kitamura et al.
732 2007; Birrell et al. 2008; Kitamura et al. 2009; Tebben et al. 2015, Quinlan et al.
733 2023). Most likely the outcome reflects a combination of molecules acting as ligands
734 for specific receptors that are expressed in competent larvae and downregulated
735 after settlement and metamorphosis. Receptors that potentially could be involved in
736 settlement cue reception and downstream signalling pathways, respectively, are G-
737 Protein coupled receptors (GPCRs) and nuclear receptors. With the help of the
738 DEView app, search terms such as “G-protein coupled receptor” or specific Pfam
739 domains can be used as filters to search the developmental transcriptome to identify
740 genes that were upregulated at competency (i.e. 93hpf) consistent with their
741 potential involvement in settlement cue perception. Searching the *Acropora* data
742 using the terms PF00104 Ligand-binding domain of nuclear hormone receptor and
743 PF00105 Zinc finger, C4 type (two domains) yielded 21 hits corresponding to 14 loci
744 (Supplementary Figure 3). Nuclear receptors play key roles in metamorphosis in
745 both insects and some vertebrates, potentially acting in the internal transmission of
746 metamorphosis signals rather than their external reception. Of the 14, seven were

upregulated at 133hpf and all of these mRNAs appear to be cleared at the 3-6hpi transition so could have roles in the cue recognition pathway and/ or metamorphosis.

The *Acropora* developmental transcriptome data, together with the DEView app, have provided novel insights into early coral development and allowed identification of candidate genes for key roles. We hope that the availability of this app via the web will lead to more extensive exploration of the data and ultimately facilitate much better understanding of the molecular processes underlying the development of the coral body plan.

For a range of organisms, including some corals, considerably more advanced genomic and transcriptomic resources are now available than could have been imagined even a few years ago. However, despite the developmental transcriptomic data provided here being to our knowledge the most comprehensive available for any coral, users need to be aware that the quality of the *Acropora millepora* dataset falls short of those available for the model invertebrates *Drosophila* and *Caenorhabditis*. Nevertheless, the developmental novelties uncovered here provide clear indications of how useful the dataset can be in facilitating coral developmental research.

Acknowledgements

The authors gratefully acknowledge the support of the Australian Research Council under Discovery Grant DP170104734, SuperScience Grant (round 2) FS110200046 and Centres of Excellence Grant CE14100020. We also thank

Gergely Torda and the staff of the Orpheus Island Research Centre for fieldwork assistance. Some of the in situ images presented here were produced by Lauretta Grasso and Nikki Hislop.

References

Aeschimann F, Neagu A, Rausch M, Großhans H. *let-7* coordinates the transition to adulthood through a single primary and four secondary targets. Life Sci Alliance. 2019; 2(2):e201900335.

Attenborough RMF, Hayward DC, Wiedemann U, Foret S, Miller DJ, Ball EE. Expression of the neuropeptides RFamide and LWamide during development of the coral Acropora millepora in relation to settlement and metamorphosis. Dev Biol. 2019; 446: 56-67.

Aviv T, Lin Z, Lau S, Rendl LM, Sicheri F, Smibert CA. The RNA-binding SAM domain of Smaug defines a new family of post-transcriptional regulators. Nat Struct Biol. 2003;10(8):614-21.

Ayers TN, Nicotra ML, Lee MT. Parallels and contrasts between the cnidarian and bilaterian maternal-to-zygotic transition are revealed in Hydractinia embryos. PLoS Genet. 2023;19(7):e1010845.

Ball EE, Hayward DC, Bridge TCL, Miller DJ. *Acropora* – the most studied coral genus. In: Boutet A, Schierwater B (eds). Handbook of Marine Model Organisms in Experimental Biology - Established and Emerging. 2021. Boca Raton (FL): CRC Press. p. 173-193. DOI: 10.1201/9781003217503-10.

Ball E, Hayward D, Reece-Hoyes J, Hislop N, Samuel G, Saint R, Harrison P and Miller, D. Coral development: from classical embryology to molecular control. Int J Dev Biol. 2002;46:671-678.

Ball EE, Hayward DC, Saint R, Miller, DJ. A simple plan—cnidarians and the origins of developmental mechanisms. Nat Rev Genetics. 2004;*5*(8):567-577.

Bamberger C, Pankow S, Yates JR 3rd. Nvp63 and nvPIWIL1 suppress retrotransposon activation in the sea anemone Nematostella vectensis. J Proteome Res. 2022; 21(11):2586-2595.

Bartel DP. MicroRNAs: genomics, biogenesis, mechanism, and function. Cell. 2022; 116(2):281-97.

Baugh LR, Hill AA, Slonim DK, Brown EL, Hunter CP. Composition and dynamics of the Caenorhabditis elegans early embryonic transcriptome. Development. 2003; 130(5):889-900.

Birrell CL, Mccook LJ, Willis BL, Harrington L. Chemical effects of macroalgae on larval settlement of the broadcast spawning coral Acropora millepora. Mar Ecol Prog Ser. 2008;362:129–137.

Bou-Abdullah F, Chasteen ND, Lesser MP. Quenching of superoxide radicals by green fluorescent protein. Biochim Biophys Acta. 2006;1760(11):1690-5.

Breitwieser FP, Baker DN, Salzberg SL. KrakenUniq: confident and fast metagenomics classification using unique k-mer counts. Genome Biol. 2018;19:198.

Chen L, Dumelie JG, Li X, Cheng MH, Yang Z, Laver JD, Siddiqui NU, Westwood JT, Morris Q, Lipshitz HD, Smibert CA. Global regulation of mRNA translation and stability in the early Drosophila embryo by the Smaug RNA-binding protein. Genome Biol. 2014;15(1):R4.

Chen S, Zhou Y, Chen Y, Gu J. fastp: an ultra-fast all-in-one FASTQ preprocessor. Bioinformatics. 2018;34:i884-i890.

Chille E, Strand E, Neder M, Schmidt V, Sherman M, Mass T, Putnam H. Developmental series of gene expression clarifies maternal mRNA provisioning and maternal-to-zygotic transition in a reef-building coral. BMC Genomics. 2021; 22(1):815.

Clarke DN, Rose NH, De Meulenaere E, Rosental B, Pearse JS, Pearse VB, Deheyn DD Fluorescent proteins generate a genetic color polymorphism and counteract oxidative stress in intertidal sea anemones. Proc Natl Acad Sci USA. 2024; 121(11):e2317017121.

Di Tommaso P, Chatzou M, Floden EW, Barja PP, Palumbo E, Notredame C. Nextflow enables reproducible computational workflows. Nat Biotechnol. 2017; 35:316-319.

854 Fridrich A, Modepalli V, Lewandowska M, Aharoni R, Moran Y.) Unravelling the
855 developmental and functional significance of an ancient Argonaute duplication. Nat
856 Commun. 2020;11(1):6187.
857
858 Gerber AP, Luschnig S, Krasnow MA, Brown PO, Herschlag D. Genome-wide
859 identification of mRNAs associated with the translational regulator PUMILIO in
860 Drosophila melanogaster. Proc Natl Acad Sci USA. 2006;103(12):4487-92.
861
862 Gilbert E, Craggs J, Modepalli V. Gene Regulatory Network that Shaped the
863 Evolution of Larval Apical Organ in Cnidaria. Mol Biol Evol. 2024;41: msad285.
864
865 Grasso L, Maindonald J, Rudd S, Hayward D, Saint R, Miller DJ, Ball EE. Microarray
866 analysis provides candidate genes for key roles in coral development. BMC
867 Genomics. 2008;9:540.
868
869 Grasso LC, Negri AP, Foret S, Hayward DC, Miller DJ, Ball EE. The biology of coral
870 metamorphosis: molecular responses of coral larvae to inducers of settlement and
871 metamorphosis. Dev Biol. 2011;353:411-419.
872
873 Gu Z, Hübschmann D. Make Interactive Complex Heatmaps in R. Bioinformatics.
874 2022;38:1460–1462. https://doi.org/10.1093/bioinformatics/btab806.
875
876 Hadfield MG. Biofilms and Marine Invertebrate Larvae: What Bacteria Produce That
877 Larvae Use to Choose Settlement Sites. Ann Rev Marine Sci. 2011;3:453-470.
878
879 Hadfield MG. Why and how marine-invertebrate larvae metamorphose so fast. Sem
880 Cell Dev Biol. 2000;11(6):437-443.
881
882 Hayward DC, Miller DJ, Ball EE. Snail expression during embryonic development of
883 the coral *Acropora*: Blurring the diploblast / triploblast divide? Development Genes
884 and Evolution. 2004;214:257-260.
885
886 Hayward DC, Samuel G, Pontynen PC, Catmull J, Saint RB, Miller DJ, Ball EE.
887 Localized expression of a DPP/BMP2-4 ortholog in a coral embryo. Proc Natl Acad
888 Sci USA. 2002;99:8106-8111.
889
890 Hayward DC, Hetherington S, Behm CA, Grasso L, Foret S, Miller DJ, Ball EE.
891 Differential gene expression at coral settlement and metamorphosis – a subtractive
892 hybridization study. PLoS One. 2011;6: e26411.
893
894 Hayward DC, Grasso LC, Saint RB, Miller DJ, Ball EE. The organizer in evolution:
895 Gastrulation and organizer gene expression highlight the importance of Brachyury
896 during development of the coral *Acropora millepora*. Dev Biol. 2015;399:227-247.
897

He S, Rangel-Huerta E, Hill E, Ellington L, Chen S, Robb S, Majerová E, Drury C, Gibson MC. An evolutionarily conserved Hox-Gbx segmentation code in the rice coral, *Montipora capitata*. bioRxiv preprint. 2024; doi: https://doi.org/10.1101/2024.09.29.615694.

Herchenröther A, Wunderlich TM, Lan J, Hake SB. Spotlight on histone H2A variants: From B to X to Z. Sem Cell Dev Biol. 2023;135:3-12.

Huffmyer AS, Wong KH, Becker DM, Strand E, Mass T, Putnam HM. Shifts and critical periods in coral metabolism reveal energetic vulnerability during development. Curr Biol. 2025;35:1-14;doi https://doi.org/10.1016/j.cub.2025.05.013.

Ishii Y, Hatta M, Deguchi R, Kawata M, Maruyama S. Gene expression alterations from reversible to irreversible stages during coral metamorphosis. Zool Lett. 2022; 8(1):4.

Iwao K, Fujisawa T, Hatta M. A cnidarian neuropeptide of the GLWamide family induces metamorphosis of reef-building corals in the genus Acropora. Coral Reefs. 2002;21:127-129.

Jessop P, Ruzov A, Gering M. Developmental Functions of the Dynamic DNA Methylome and Hydroxymethylome in the Mouse and Zebrafish: Similarities and Differences. Front Cell Dev Biol. 2018;20(6):27.

Jones P, Binns D, Chang HY, Fraser M, Li W, McAnulla C, McWilliam H, Maslen J, Mitchell A, Nuka G, Pesseat S. InterProScan 5: genome-scale protein function classification. Bioinformatics. 2014;30(9):1236-40.

Kitamura M, Koyama T, Nakano Y, Uemura D. Characterization of a natural inducer of coral larval metamorphosis. J Exp Mar Biol Ecol. 2007;340:96-102.

Kitamura M, Schupp PJ, Nakano Y, Uemura D. Luminaolide, a novel metamorphosis-enhancing macrodiolide for scleractinian coral larvae from crustose coralline algae. Tetrahedron Letts. 2009;50:6606-6609.

Langfelder P, Horvath S. WGCNA: an R package for weighted correlation network analysis. BMC Bioinformatics. 2008;9:559. https://doi.org/10.1186/1471-2105-9-559.

Langmead B, Salzberg SL. Fast gapped-read alignment with Bowtie 2. Nat Methods. 2012;9:357-359.

Levy S, Elek A, Grau-Bové X, Menéndez-Bravo S, Iglesias M, Tanay A, Mass T, Sebé-Pedrós A. A stony coral cell atlas illuminates the molecular and cellular basis of coral symbiosis, calcification, and immunity. Cell. 2021;184(11):2973-2987.

Li B, Dewey CN. RSEM: accurate transcript quantification from RNA-Seq data with or without a reference genome. BMC Bioinformatics. 2011;12:323.

Lorković ZJ, Berger F. Heterochromatin and DNA damage repair: Use different histone variants and relax. Nucleus. 2017;8(6):583-588.

Love MI, Huber W, Anders S. Moderated estimation of fold change and dispersion for RNA-seq data with DESeq2. Genome Biol. 2014;15:550.

Mansour TA, Rosenthal JJ, Brown CT, Roberson LM. Transcriptome of the Caribbean stony coral Porites astreoides from three developmental stages. Gigascience. 2016;5(1):33.

Mason BM, Cohen JH. Long-wavelength photosensitivity in coral planula larvae. Biol Bull. 2012;222(2):88-92.

Mason B, Cooke I, Moya A, Augustin R, Lin M-F, Satoh N, Bosch TCG, Bourne DG, Hayward DC, Andrade N, Forêt S, Ying H, Ball EE, Miller DJ. AmAMP1 from *Acropora millepora* and damicornin define a family of coral-specific antimicrobial peptides related to the Shk toxins of sea anemones. Dev Comp Immunol. 2021;114: 103866.

Mason B, Hayward DC, Moya A, Cooke I, Sorenson A, Brunner R, Andrade N, Huerlimann R, Bourne DG, Schaeffer P, Grinblat M, Ravasi T, Ueda N, Tang SL, Ball EE, Miller DJ. Microbiome manipulation by corals and other Cnidaria via quorum quenching. Curr Biol. 2024;34(14):3226-3232.e5.

Mason BM, Koyanagi M, Sugihara T, Iwasaki M, Slepak V, Miller DJ, Sakai Y, Terakita A. Multiple opsins in a reef-building coral, *Acropora millepora*. Scientific Reports 2023;23:1628.

Matsumoto N, Sato K, Nishimasu H, Namba Y, Miyakubi K, Dohmae N, Ishitani R, Siomi H, Siomi MC, Nureki O. Crystal structure and activity of the endoribonuclease domain of the piRNA pathway factor Maelstrom. Cell Reps. 2015;11:366-375.

Mazza ME, Pang K, Reitzel AM, Martindale MQ, Finnerty JR. A conserved cluster of three PRD-class homeobox genes (homeobrain, rx and orthopedia) in the Cnidaria and Protostomia. EvoDevo. 2010;1:1-15.

Meyer E, Aglyamova GV, Matz MV. Profiling gene expression responses of coral larvae (Acropora millepora) to elevated temperature and settlement inducers using a novel RNA-Seq procedure. Mol Ecol. 2011;20:3599-616.

Meyer E, Aglyamova GV, Wang S, Buchanan-Carter J, Abrego D, Colbourne JK, Willis BL, Matz MV. Sequencing and de novo analysis of a coral larval transcriptome using 454 GSFlx. BMC Genomics. 2009;10:1-8.

Michail C, Rodrigues Lima F, Viguier M, Deshayes F. Structure and function of the lysine methyltransferase SETD2 in cancer: From histones to cytoskeleton**.** Neoplasia. 2025;59:101090.

Miller DJ, Hemmrich G, Ball EE, Hayward DC, Khalturin K, Funayama N, Agata K, Bosch TCG.The innate immune repertoire in Cnidaria – ancestral complexity and stochastic gene loss. Genome Biol. 2007;8:R59.

Mishima Y, Tomari Y. Pervasive yet nonuniform contributions of Dcp2 and Cnot7 to maternal mRNA clearance in zebrafish. Genes Cells. 2017;22(7):670-678.

Modepalli V, Fridrich A, Agron M, Moran Y. The methyltransferase HEN1 is required in Nematostella vectensis for microRNA and piRNA stability as well as larval metamorphosis. PLoS Genet. 2018;14(8):e1007590.

Mohr F, Döhner K, Buske C, Rawat VP. TET genes: new players in DNA demethylation and important determinants for stemness. Exp Hematol. 2011; 39(3):272-81.

Moran Y, Agron M, Praher D, Technau U. The evolutionary origin of plant and animal microRNAs. Nat Ecol Evol. 2017;1(3):27.

Morse DE, Hooker N, Morse AN, Jensen RA. Control of larval metamorphosis and recruitment in sympatric agariciid corals. J Exp Mar Biol Ecol. 1988;116(3):193-217.

Negri AP, Webster NS, Hill RT, Heyward AJ. Metamorphosis of broadcast spawning corals in response to bacteria isolated from crustose algae. Mar Ecol Prog Ser. 2001;*223*:121-131.

Okubo N, Hayward DC, Forêt S, Ball EE. A comparative view of early development in the corals *Favia lizardensis*, *Ctenactis echinata*, and *Acropora millepora* - morphology, transcriptome, and developmental gene expression. BMC Evol Biol. 2016;16:1-12.

Okubo N, Mezaki T, Nozawa Y, Nakano Y, Lien YT, Fukami H, Hayward DC, Ball EE Comparative embryology of eleven species of stony corals (Scleractinia). PLoS One. 2013;8(12): e84115.

Osakabe A, Molaro A Histone renegades: Unusual H2A histone variants in plants and animals. Sem Cell Dev Biol. 2023;135:35-42.

Palmer CV, Modi CK, Mydlarz LD. Coral fluorescent proteins as antioxidants. PLoS One. 2009;4(10):e7298.

Praher D, Zimmermann B, Genikhovich G, Columbus-Shenkar Y, Modepalli V, Aharoni R, Moran Y, Technau U. Characterization of the piRNA pathway during development of the sea anemone Nematostella vectensis. RNA Biol. 2017; 14(12):1727-1741.

Quinlan ZA, Bennett MJ, Arts MGI, Levenstein M, Flores D, Tholen HM, Tichy L, Juarez G, Haas AF, Chamberland VF, Latijnhouwers KRW, Vermeij MJA, Johnson AW, Marhaver KL, Kelly LW. Coral larval settlement induction using tissue-associated and exuded coralline algae metabolites and the identification of putative chemical cues. Proc Roy Soc B. 2023;290:20231476. https://doi.org/10.1098/rspb.2023.1476.

Rabani M, Pieper L, Chew G-L, Schier AH. A Massively Parallel Reporter Assay of 3' UTR Sequences Identifies In Vivo Rules for mRNA Degradation. Mol Cell. 2017; 68(6):1083-1094.e5.

Reyes-Bermudez A, Desalvo MK, Voolstra CR, Sunagawa S, Szmant AM, Iglesias-Prieto R, Medina M. Gene expression microarray analysis encompassing metamorphosis and the onset of calcification in the scleractinian coral Montastraea faveolata. Mar Genomics 2009;2:149-159.

Ramon-Mateu J, Ferraioli A, Teixidó N, Domart-Coulon I, Houliston E, Copley RR. Aboral cell types of Clytia and coral larvae have shared features and link taurine to the regulation of settlement. Science Adv. 2025;16;11(20):eadv1159.

Reyes-Bermudez A, Villar-Briones A, Ramirez-Portilla C, Hidaka M, Mikheyev AS Developmental Progression in the Coral *Acropora digitifera* Is Controlled by Differential Expression of Distinct Regulatory Gene Networks. Genome Biol Evol. 2016;8(3):851-70.

Salih A, Larkum A, Cox G, Kuhl M, Hoegh-Guldberg Fluorescent pigments in corals are photoprotective. Nature.2000;408:850-853.

Shoguchi E, Beedessee G, Hisata K, Tada I, Narisoko H, Satoh N, Kawachi M, Shinzato C. A New Dinoflagellate Genome Illuminates a Conserved Gene Cluster Involved in Sunscreen Biosynthesis. Genome Biol Evol. 2021;13:evaa235.

Sato K, Siomi MC. Functional and structural insights into the piRNA factor Maelstrom. FEBS Lett. 2015;589:1688-1693.

Siboni N, Abrego D, Puill-Stephan E, King WL, Bourne DG, Raina J-B, Seymour JR, Harder T. Crustose coralline algae that promote coral larval settlement harbor distinct surface bacterial communities. Coral Reefs 2020;39:1703–1713.

Spike CA, Tsukamoto T, Greenstein D. Ubiquitin ligases and a processive proteasome facilitate protein clearance during the oocyte-to-embryo transition in *Caenorhabditis elegans*. Genetics. 2022;221(1):iyac051.

Strader ME, Davies SW, Matz MV (2015) Differential responses of coral larvae to the colour of ambient light guide them to suitable settlement microhabitat. R Soc Open Sci 2(10):150358

Strader ME, Aglyamova GV, Matz MV. Molecular characterization of larval development from fertilization to metamorphosis in a reef-building coral. BMC Genomics. 2018;19(1):1-17.

Takeuchi T, Yamada L, Shinzato C, Sawada H, Satoh N. Stepwise Evolution of Coral Biomineralization Revealed with Genome-Wide Proteomics and Transcriptomics. PLoS One 2016;11(6):e0156424.

Tebben J, Motti CA, Siboni N, Tapiolas DM, Negri AP, Schupp PJ, Kitamura M, Hatta M, Steinberg PD, Harder T. Chemical mediation of coral larval settlement by crustose coralline algae. Sci Rep. 2015;5:10803.

Technau U. Gastrulation and germ layer formation in the sea anemone Nematostella vectensis and other cnidarians. Mech Dev. 2020;163:103628.

Török A, Schiffer PH, Schnitzler CE, Ford K, Mullikin JC, Baxevanis AD, Bacic A, Frank U, Gornik SG. The cnidarian Hydractinia echinata employs canonical and highly adapted histones to pack its DNA. Epigenetics Chromatin. 2016;9(1):1-17.

Tran C, Hadfield MG. Are G-protein-coupled receptors involved in mediating larval settlement and metamorphosis of coral planulae? Biol Bull 2012;222(2):128-36.

Turnlund AC, Vanwonterghem I, Botté ES, Randall CJ, Giuliano C, Kam L, Bell S, O'Brien P, Negri AP, Webster NS, Lurgi M. Linking differences in microbial network structure with changes in coral larval settlement. ISME Comm. 2023;3:114.

Vastenhouw NL, Cao WX, Lipshitz HD. The maternal-to-zygotic transition revisited. Development. 2019;146(11): dev161471

Walker NS, Fernández R, Sneed JM, Paul VJ, Giribet G, Combosch DJ. Differential gene expression during substrate probing in larvae of the Caribbean coral *Porites astreoides*. Mol Ecol. 2019;28(22):4899-4913.

Wickham H. Data Analysis, in: Wickham, H. (Ed.), Ggplot2: Elegant Graphics for Data Analysis. Springer International Publishing, Cham, 2016; pp. 189–201. https://doi.org/10.1007/978-3-319-24277-4_9.

Wu X, Zhang Y. TET-mediated active DNA demethylation: mechanism, function and beyond. Nat Rev Genet. 2017;18(9):517-534.

Yasuoka Y, Shinzato C, Satoh N. The Mesoderm-Forming Gene brachyury Regulates Ectoderm-Endoderm Demarcation in the Coral Acropora digitifera. Curr Biol. 2016;26(21):2885-2892.

Availability of data and materials

Data accessibility statement: To facilitate use and rapid exploration of the *Acropora millepora* developmental transcriptome we created an interactive web application that is hosted on servers provided by the Australian Research Data Commons Nectar Research Cloud to ensure that it is scalable and highly available for long-term use. Users can access the web application directly at https://amil-deview.mmb.group or obtain its source code and the underlying data from our github repository (https://github.com/iracooke/amil2_dev).

Author Contributions

Designed research: AM, DH, BL, EB, DM
Carried out field work: AM, DH, BL, EB
Laboratory work: AM, BL
Performed bioinformatic analyses: SF, AM, DH, IC
Contributed new analytical tools: IC
Analysed the data: AM, RB, MG, DH, DM
Wrote the paper: DH, RB, EB, IC, DM (lead)

Figure legends

1154

1155 Figure 1. Images showing the morphologies recorded at the time of collection at the
1156 timepoints indicated. Times are given in hours post fertilisation (hpf) and hours post
1157 induction (hpi). The places in the developmental sequence of two major events,
1158 gastrulation and induction with a settlement cue, are indicated. Some of the SEM
1159 images have been previously published in Grasso et al. 2008, Hayward et al. 2011,
1160 and Ball et al. 2021.

1161

1162 Figure 2. PCA analysis of the developmental transcriptomic data. Principal
1163 Components Analysis (PCA) of the developmental transcriptome data with ellipses
1164 representing 95% confidence levels. At 93 hours post fertilisation (hpf), larvae were
1165 competent to settle in response to ethanolic CCA extract and settlement was
1166 induced at the age of 133hpf. Settlement induction caused larvae to elongate at 15
1167 minutes post induction (mpi) and 100% of larvae had initiated metamorphosis at 3
1168 hours post induction (hpi). A major change in gene expression occurred between 3
1169 and 6hpi.

1170

1171 Figure 3. Serial up-down expression plots showing the number of genes changing in
1172 expression between consecutive time points during development. There are three
1173 periods that show major changes in expression: early development leading up to
1174 gastrulation (5-29hpf), 81-133hpf as competence to settle is developing, and 3-6hpi
1175 as polyp development is getting under way after settlement.

1176

1177 Figure 4. Expression of histone genes and histone modifying enzymes during the
1178 early development of *Acropora millepora*. (A) Heatmap showing expression of
1179 selected histone genes during development. mRNAs encoding canonical histones
1180 H3, H4 and H2B are present at high levels in eggs (rows 3, 4 and 5 from the top), as
1181 are H2A.X and H2A.V (but not canonical H2A) messages. Zygotic expression of the
1182 four core canonical histones begins at the start of gastrulation (i.e. the 13hpf time
1183 point) note that the set of histone genes shown in the bottom four rows are likely to
1184 represent a replication-dependent subset that may be required at high levels only
1185 early in development. Consistent with this, the top row shows data for another H2A
1186 gene, expression of which begins later in development. (B) Heatmap showing
1187 expression of histone modifying enzymes during the early development of *Acropora*.

1188 mRNAs encoding the histone acetyltransferase KAT6A the histone H3K36
1189 methylase SETD2 are maternal (rows 2 and 3, respectively). Two other histone
1190 acetyltransferases (HAC5 and KAT5; top and bottom rows) are most highly
1191 expressed at the 6hpi time point, reflecting their possible role in activating chromatin
1192 during the post-settlement transition. Note that a second wave of expression of both
1193 KAT6A and SETD2 also occurs at that time.
1194
1195 Figure 5. Heatmaps and in situ hybridisation provide complementary data, as
1196 illustrated by data for coral homologs of the *Drosophila* genes, snail and homeobrain.
1197 During gastrulation, these genes have complementary morphological expression
1198 patterns, *Am-snail* marking the presumptive mesendoderm (Hayward et al. 2004)
1199 and *Am-homeobrain* the presumptive ectoderm. (A) Diagrammatic vertical sections
1200 of embryos aged from early prawn chip to sphere. (B-D) Embryos aged from prawn
1201 chip to sphere (blastopore closure) viewed in three different ways. (B) Critical-point
1202 dried embryos viewed with scanning electron microscopy reveal the external
1203 morphology, (C) Whole mount in situ hybridisation reveals the spatial expression of
1204 *Am-snail*. (D) Vertical sections of in situ preparations reveal the internal distribution
1205 of the expressing tissue in the developing mesendoderm. (E) Expression of *Am-*
1206 *homeobrain* in the developing ectoderm revealed using whole-mount in situ
1207 hybridisation. Note that the two genes are complimentary in their expression. (C', E')
1208 Heatmap showing the relative expression of the two corresponding genes over the
1209 course of development. Parts of the figure were published in Hayward et al. (2004)
1210 Development Genes & Evolution 214:257-260, Springer Nature.
1211
1212 Figure 6. In situ hybridisation and heatmaps provide complementary data in support
1213 of roles for known and suspected anti-bacterial activities during settlement and
1214 metamorphosis in *Acropora*. The upper three rows show in situ hybridisation data for
1215 developmental stages leading into and immediately following settlement for (A) the
1216 anti-microbial protein AmAMP1 (Mason et al. (2021), (B) the quorum quenching
1217 activity AmNtNH1 (Mason et al. 2024), and (C) the MAC-Perforin protein Apextrin
1218 Miller et al. 2007; Hayward et al. 2011). A', B' and C' are heatmaps showing the
1219 corresponding temporal expression levels of the three genes. The arrowheads
1220 indicate the time of settlement induction.
1221

1222 Figure 7. Heatmaps for genes implicated in (A) DNA methylation /demethylation and
1223 (B) clearance of mRNAs and proteins are consistent with major changes in gene
1224 activity occurring at 3-6hpi. The upper panel (A) illustrates relative expression levels
1225 of the *Acropora* homologs of ten-eleven-translocase (tet), the primary role of which is
1226 removal of CpG methylation marks, the de novo DNA methyltransferase, DNMT3,
1227 and the maintenance DNA methyltransferase, DNMT1. Although all three activities
1228 are expressed during gastrulation, TET is most heavily expressed at the 6hpi time
1229 point. The lower panel (B) shows relative expression levels of *Acropora* homologs of
1230 the conserved mRNA clearance activities, Smaug and Pumilio, and the TRIM-NHL
1231 ubiquitin ligase, TRIM71/LIN41. Smaug and TRIM71/LIN41are most heavily
1232 expressed at the 6hpi time point; three gene predictions annotated as Pumilio
1233 homologs (corresponding to at least two distinct gene products) were also up-
1234 regulated at that time.
1235
1236 Figure 8. Expression of genes involved in small RNA (miRNA and piRNA)
1237 processing during early development. mRNAs encoding HEN1 and Dicer homologs
1238 (rows 6 and 7) were present at high levels in eggs, as were those encoding
1239 homologs of Maelstrom, Vasa/DDX4.1 and .2, and Piwi2, which function primarily in
1240 piRNA-mediated transposon silencing. Other miRNA processing activities, including
1241 homologs of Serrate/SRRT and DGCR8/Pasha, were also expressed in embryos,
1242 larvae and during post settlement life, implying extensive involvement of miRNAs in
1243 regulating gene activities during early coral development.
1244
1245 Supplementary Figure 1.
1246 Weighted gene co-expression network analysis (WGCNA) clustered the
1247 developmental gene expression data into 39 modules based on correlated
1248 expression patterns. The number of genes in each module range from 18 (plum
1249 module) to 5851 (turquoise module) and the grey module contains all genes that did
1250 not fit into any other module. The WGCNA heatmap indicated that there is a major
1251 change in gene expression between 3 and 6 hours post induction (hpi) and also
1252 showed that settlement induction at the age of 133 hours post fertilisation (hpf) did
1253 not trigger an immediate strong change in gene expression 15 minutes post
1254 induction (mpi).
1255

1256 Supplementary Figure 2.
1257 Genes previously characterised in the context of gastrulation illustrate the need for
1258 spatial as well as temporal expression data. In situ data for the *Acropora* homologs
1259 of several genes imply conservation of function during gastrulation with Bilateria. (A)
1260 BMP2/4 (BMP2B), (B) Forkhead (FOXA2), (C) Goosecoid (GSC) and (D) Brachyury
1261 (TBXT). However, heatmaps show that, for most of these genes, rather than at
1262 gastrulation (around 13 – 18 hpf) the expression maxima occur post-settlement. Only
1263 one of the genes characterised in the context of gastrulation (snail) has a major peak
1264 of expression at the late “prawn chip” (gastrula) stage (Figure 5) – which is
1265 consistent with in situ data (Hayward et al. 2004) suggesting expression throughout
1266 the presumptive mesendoderm. The in situs were previously published in Hayward
1267 et al. (2015) Developmental Biology 399:337-347 (Elsevier).
1268
1269
1270 Supplementary Figure 3.
1271 Differential expression of genes encoding nuclear receptors during coral
1272 development. Searching the *Acropora* data using the terms PF00104 Ligand-binding
1273 domain of nuclear hormone receptor and PF00105 Zinc finger, C4 type (two
1274 domains) yielded hits corresponding to 14 loci. Two of these loci code for predicted
1275 protein isoforms with distinct expression profiles (XP_029208454.1 and
1276 XP_029208455.1 are protein isoforms from the locus LOC114972094;
1277 XP_044184859.1 and XP_044184860.1 are isoforms from the locus
1278 LOC114969161). Consistent with possible roles in cue recognition and/ or
1279 metamorphosis, seven of the 14 genes were upregulated at 133hpf. All of these
1280 mRNAs were cleared at the 3-6hpi transition.
1281

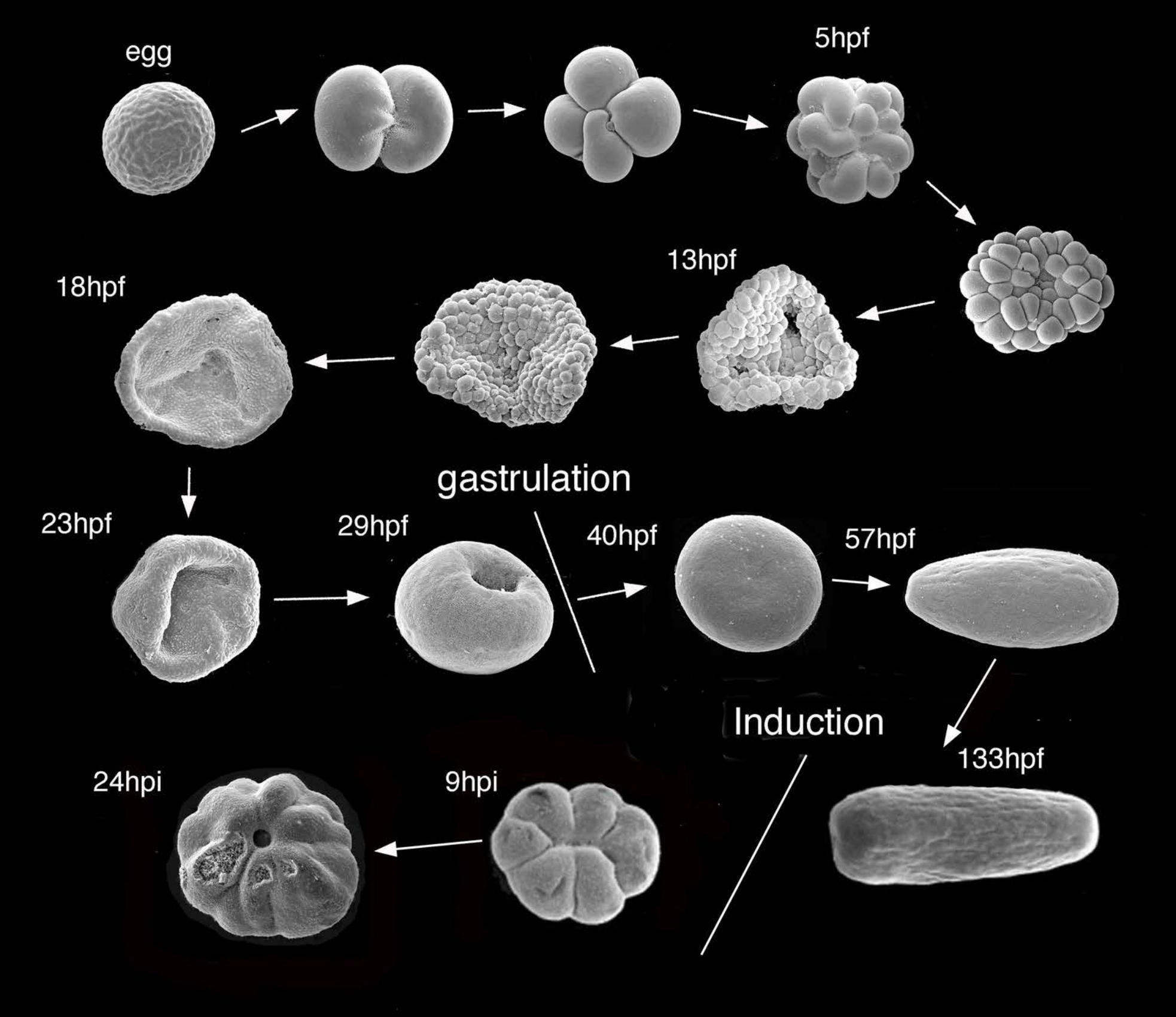
egg
5hpf
13hpf
18hpf
gastrulation
23hpf
29hpf
40hpf
57hpf
Induction
133hpf
24hpi
9hpi

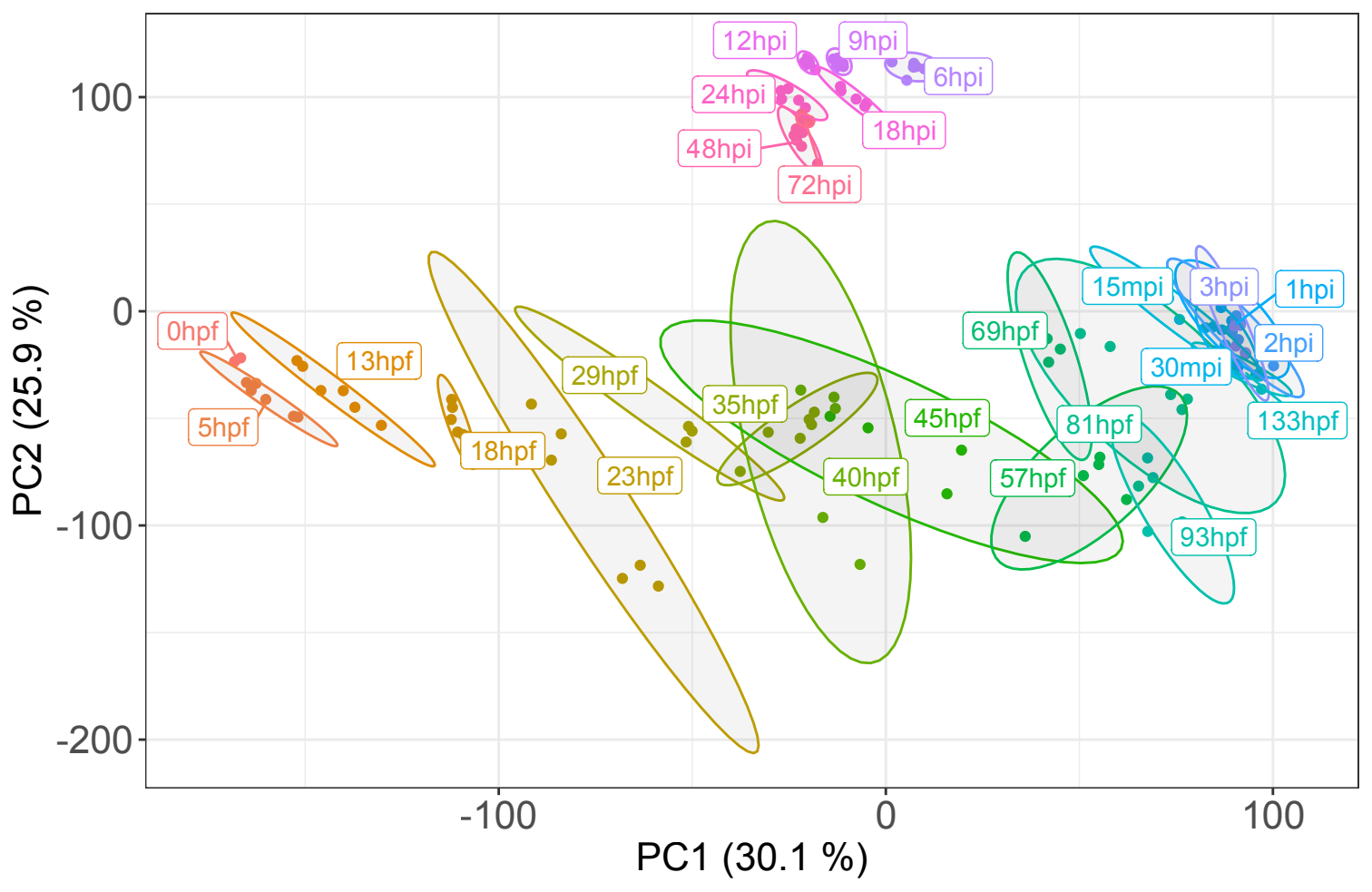
12hpi
9hpi
6hpi
24hpi
18hpi
48hpi
72hpi
0hpf
13hpf
5hpf
18hpf
29hpf
23hpf
35hpf
40hpf
45hpf
69hpf
57hpf
81hpf
93hpf
15mpi
3hpi
1hpi
2hpi
30mpi
133hpf
100
0
-100
-200
-100
0
100
PC2 (25.9 %)
PC1 (30.1 %)

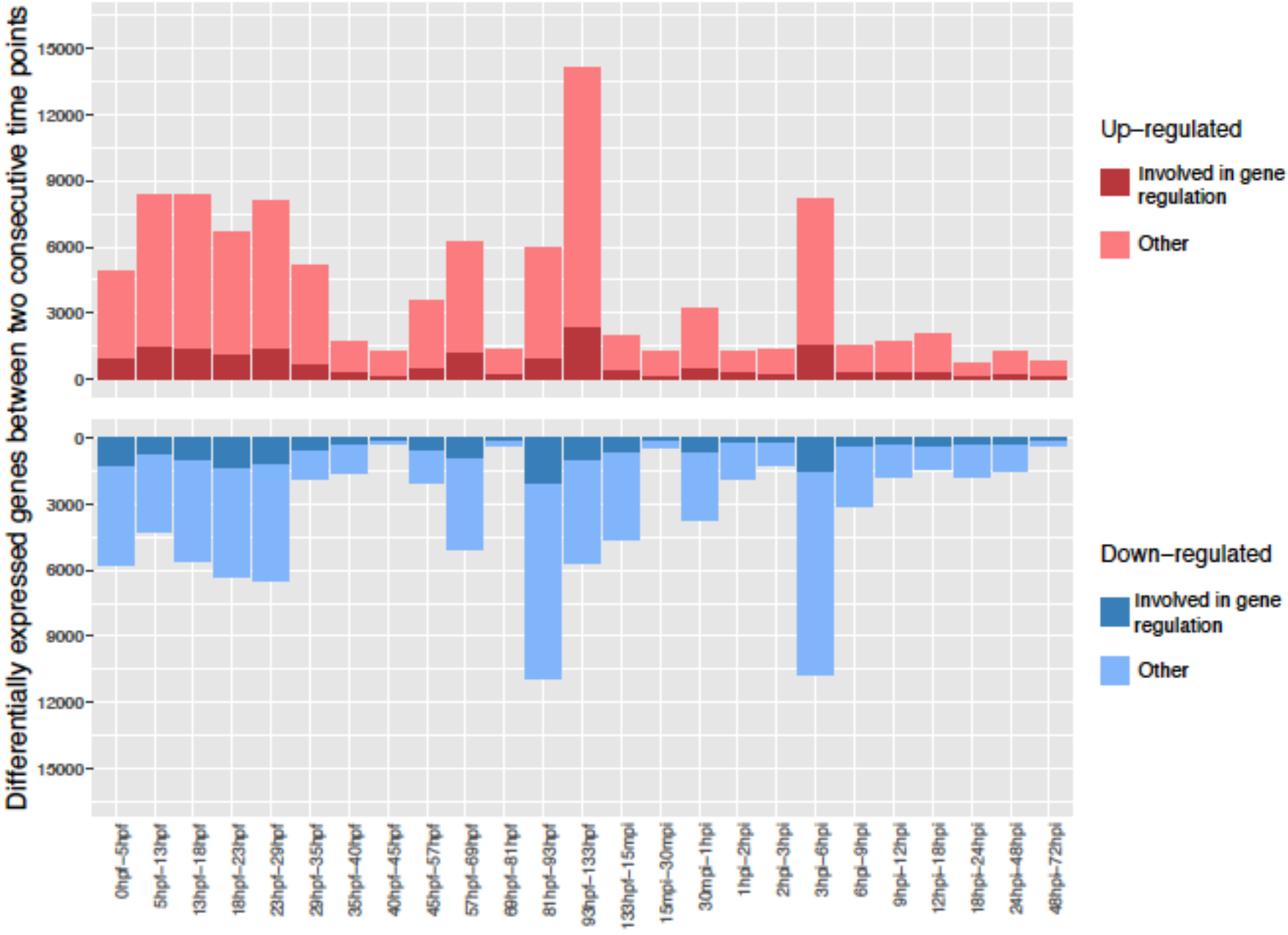
Differentially expressed genes between two consecutive time points
15000
12000
9000
6000
3000
0
Up−regulated
Involved in gene regulation
Other
Down−regulated
Involved in gene regulation
Other
0hpf−5hpf
5hpf−13hpf
13hpf−18hpf
18hpf−23hpf
23hpf−29hpf
29hpf−35hpf
35hpf−40hpf
40hpf−45hpf
45hpf−57hpf
57hpf−69hpf
69hpf−81hpf
81hpf−93hpf
93hpf−133hpf
133hpf−15mpi
15mpi−30mpi
30mpi−1hpi
1hpi−2hpi
2hpi−3hpi
3hpi−6hpi
6hpi−9hpi
9hpi−12hpi
12hpi−18hpi
18hpi−24hpi
24hpi−48hpi
48hpi−72hpi

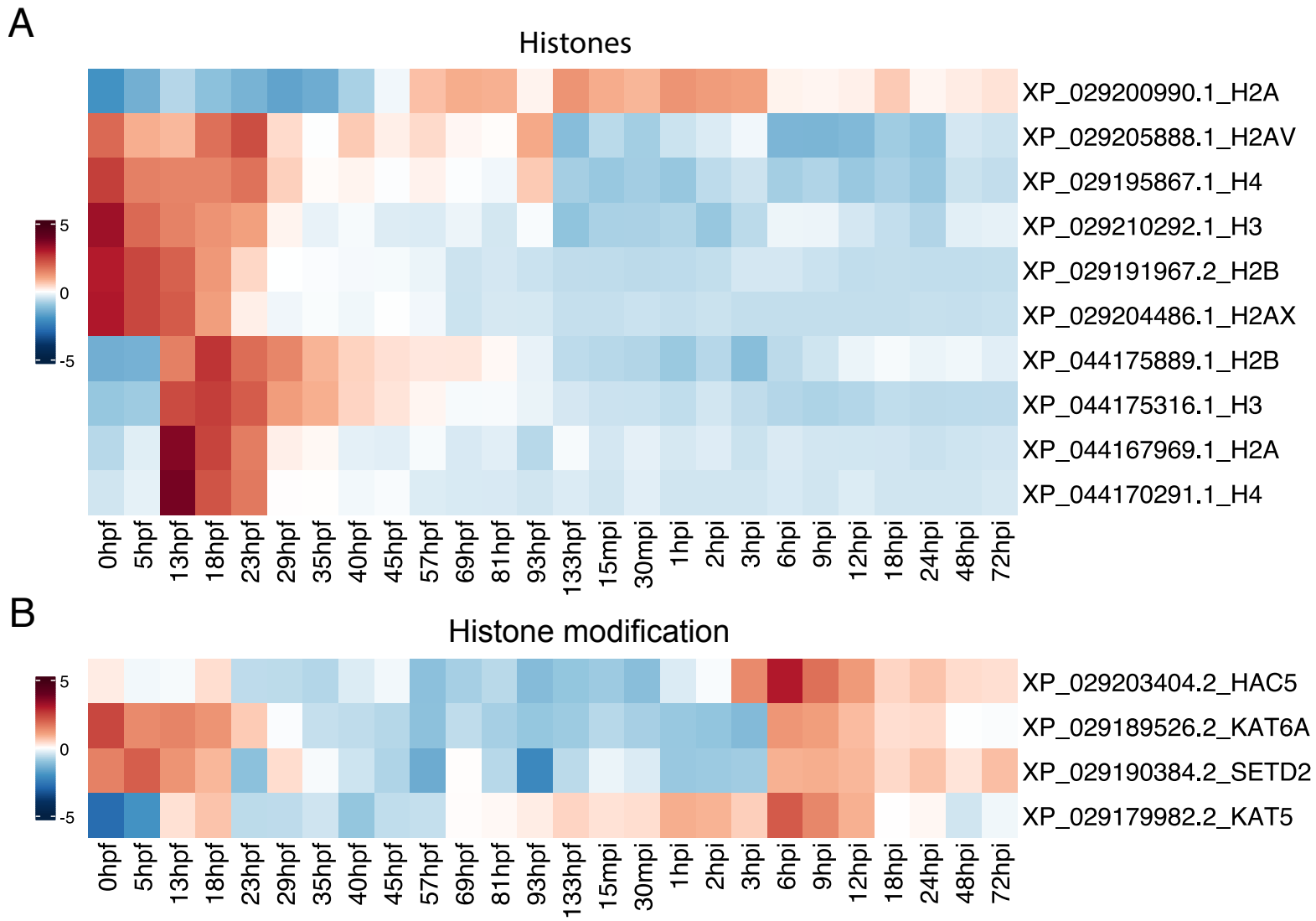
A
Histones
XP_029200990.1_H2A
XP_029205888.1_H2AV
XP_029195867.1_H4
XP_029210292.1_H3
XP_029191967.2_H2B
XP_029204486.1_H2AX
XP_044175889.1_H2B
XP_044175316.1_H3
XP_044167969.1_H2A
XP_044170291.1_H4
5
0
-5
0hpf
5hpf
13hpf
18hpf
23hpf
29hpf
35hpf
40hpf
45hpf
57hpf
69hpf
81hpf
93hpf
133hpf
15mpi
30mpi
1hpi
2hpi
3hpi
6hpi
9hpi
12hpi
18hpi
24hpi
48hpi
72hpi
B
Histone modification
XP_029203404.2_HAC5
XP_029189526.2_KAT6A
XP_029190384.2_SETD2
XP_029179982.2_KAT5
5
0
-5
0hpf
5hpf
13hpf
18hpf
23hpf
29hpf
35hpf
40hpf
45hpf
57hpf
69hpf
81hpf
93hpf
133hpf
15mpi
30mpi
1hpi
2hpi
3hpi
6hpi
9hpi
12hpi
18hpi
24hpi
48hpi
72hpi

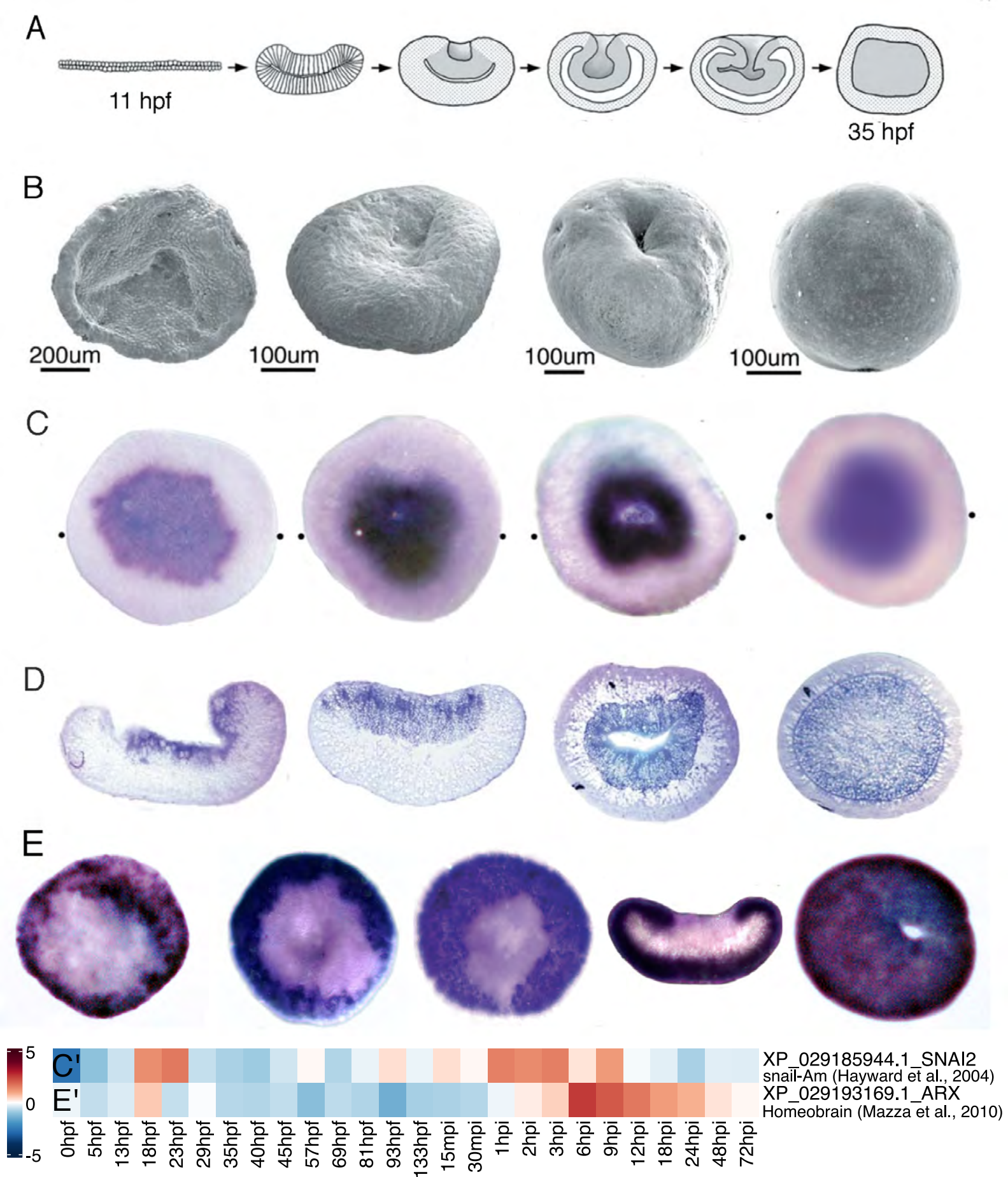
A
11 hpf
35 hpf
B
200um
100um
100um
100um
C
D
E
5
0
-5
C'
E'
0hpf
5hpf
13hpf
18hpf
23hpf
29hpf
35hpf
40hpf
45hpf
57hpf
69hpf
81hpf
93hpf
133hpf
15mpi
30mpi
1hpi
2hpi
3hpi
6hpi
9hpi
12hpi
18hpi
24hpi
48hpi
72hpi
XP_029185944.1_SNAI2
snail-Am (Hayward et al., 2004)
XP_029193169.1_ARX
Homeobrain (Mazza et al., 2010)

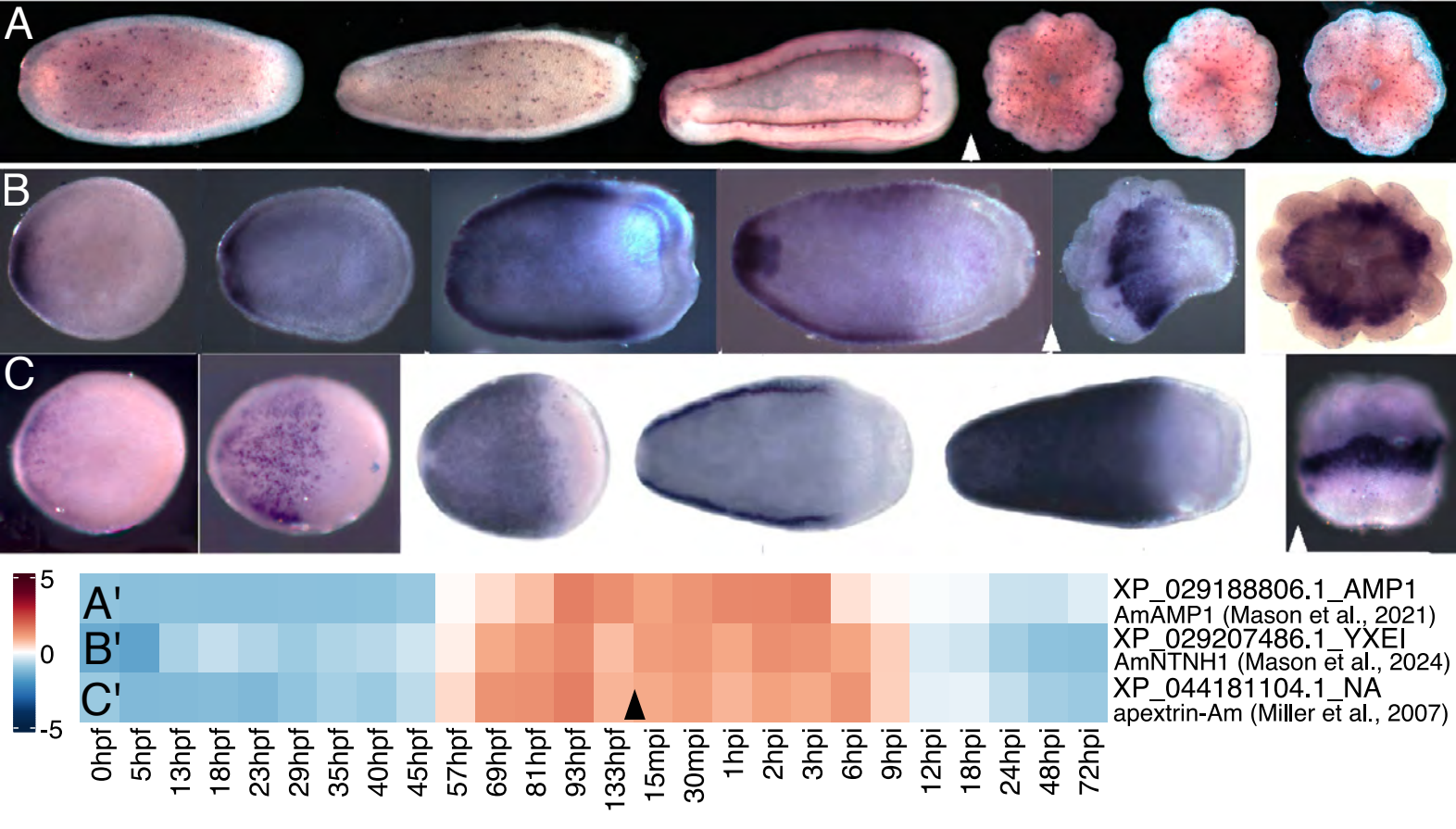
A
B
C
5
0
-5
A'
B'
C'
XP_029188806.1_AMP1
AmAMP1 (Mason et al., 2021)
XP_029207486.1_YXEI
AmNTNH1 (Mason et al., 2024)
XP_044181104.1_NA
apextrin-Am (Miller et al., 2007)
0hpf
5hpf
13hpf
18hpf
23hpf
29hpf
35hpf
40hpf
45hpf
57hpf
69hpf
81hpf
93hpf
133hpf
15mpi
30mpi
1hpi
2hpi
3hpi
6hpi
9hpi
12hpi
18hpi
24hpi
48hpi
72hpi

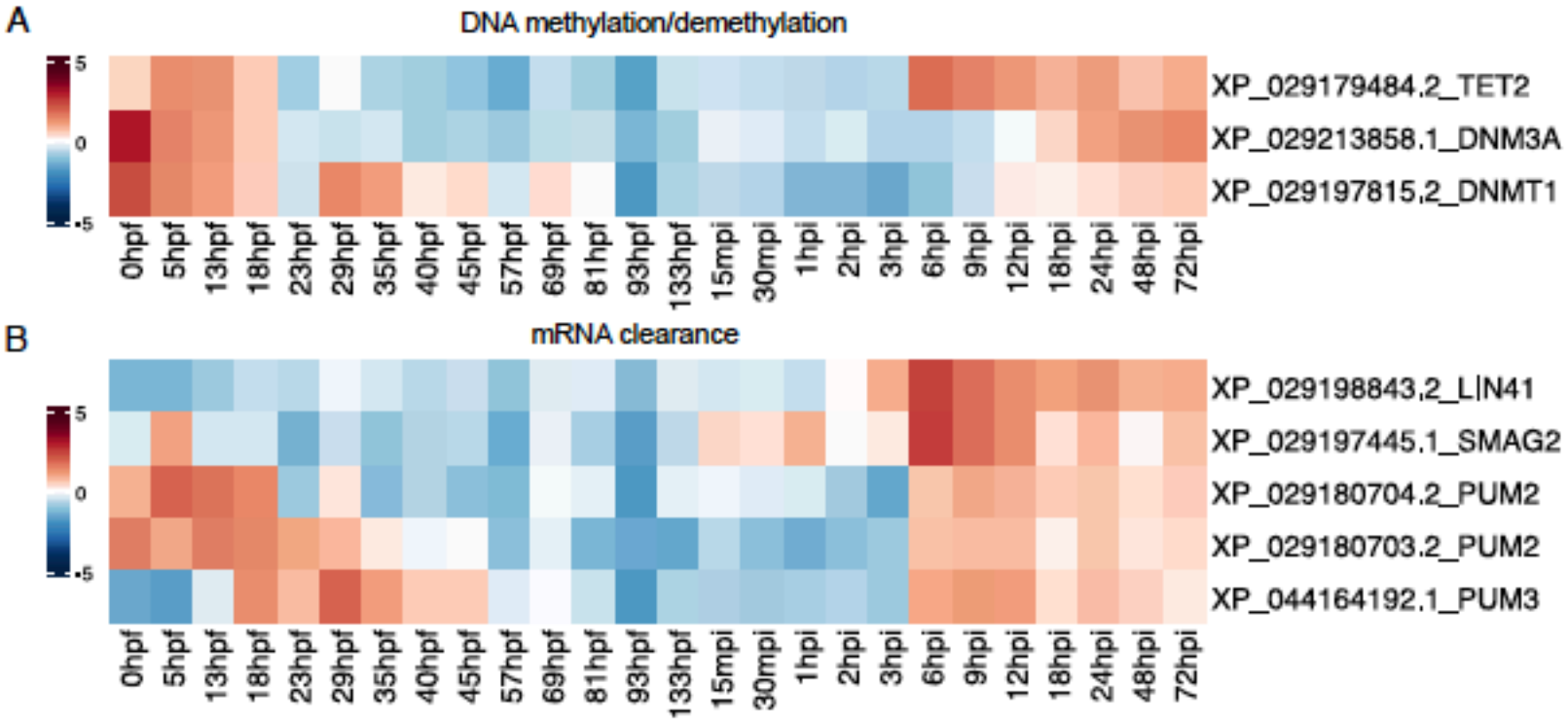
A
DNA methylation/demethylation
5
0
-5
XP_029179484.2_TET2
XP_029213858.1_DNM3A
XP_029197815.2_DNMT1
0hpf
5hpf
13hpf
18hpf
23hpf
29hpf
35hpf
40hpf
45hpf
57hpf
69hpf
81hpf
93hpf
133hpf
15mpi
30mpi
1hpi
2hpi
3hpi
6hpi
9hpi
12hpi
18hpi
24hpi
48hpi
72hpi
B
mRNA clearance
5
0
-5
XP_029198843.2_LIN41
XP_029197445.1_SMAG2
XP_029180704.2_PUM2
XP_029180703.2_PUM2
XP_044164192.1_PUM3
0hpf
5hpf
13hpf
18hpf
23hpf
29hpf
35hpf
40hpf
45hpf
57hpf
69hpf
81hpf
93hpf
133hpf
15mpi
30mpi
1hpi
2hpi
3hpi
6hpi
9hpi
12hpi
18hpi
24hpi
48hpi
72hpi

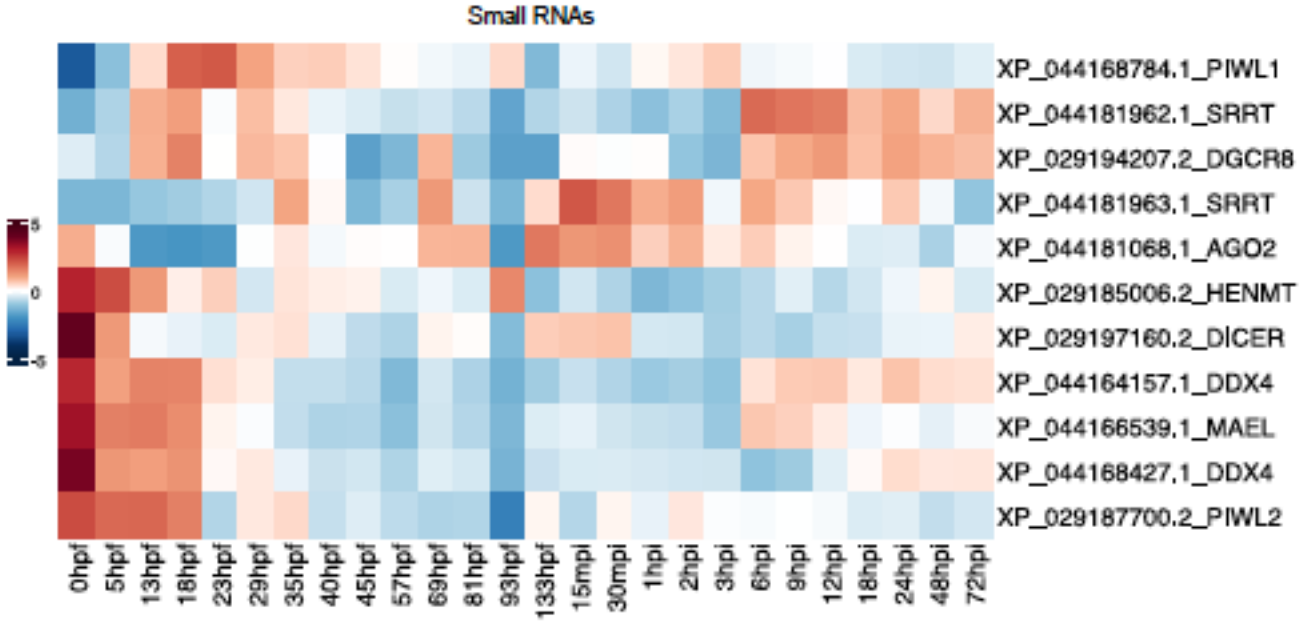
Small RNAs
XP_044168784.1_PIWL1
XP_044181962.1_SRRT
XP_029194207.2_DGCR8
XP_044181963.1_SRRT
XP_044181068.1_AGO2
XP_029185006.2_HENMT
XP_029197160.2_DICER
XP_044164157.1_DDX4
XP_044166539.1_MAEL
XP_044168427.1_DDX4
XP_029187700.2_PIWL2
5
0
-5
0hpf
5hpf
13hpf
18hpf
23hpf
29hpf
35hpf
40hpf
45hpf
57hpf
69hpf
81hpf
93hpf
133hpf
15mpi
30mpi
1hpi
2hpi
3hpi
6hpi
9hpi
12hpi
18hpi
24hpi
48hpi
72hpi

Table 1. Previous studies on the molecular bases of early development in hard corals

Coral species	Reference	Stages sampled						Focus of study	Methodology*
Acropora millepora									
	Grasso et al., 2008	prawn chip 8 hpf	planula 83 hpf	primary polyp 130 hpf	adult			Early survey of developmental changes	ESTs
	Grasso et al., 2011	egg (unfertilised)	prawn chip 8 hpf	planula 83 hpf	primary polyp 130 hpf	adult		Pre- vs post-settlement	ESTs
	Hayward et al., 2011			planula	primary polyp			Pre vs post settlement	SSH
	Strader et al., 2018	22 hpf	46 hpf	73 hpf	89 hpf	24 hour intervals		Competence and fluorescence	
Acropora digitifera									
	Takeuchi et al., 2016	egg	blastula	gastrula	larva	meta	adult	Calcification genes	
	Reyes-Bermudez et al., 2016	prawn chip 12 hpf	gastrula 24 hpf	sphere 48 hpf	planula 96 hpf	adult		Stage specific transcript profiles	
Acropora tenuis									
	Ishii et al. 2022	0, 1 and 6 hr post induction						Commitment to settlement	
Montipora capitata									
	Chillie et al., 2021	0 hpf (egg) (Unfertilised)	1 hpf	4hpf	9hpf	14hpf	22hpf	Maternal-zygotic transition	
	He et al., 2024	0 hpf (egg) (unfertilised?)	prawn chip 14hpf	sphere 38hpf	pear 62hpf	86hpf	planula 110hpf	Developmental roles of Hox-Gbx genes	
	Huffmyer et al., 2025	Egg (fertilised) 1hpf	cleavage 5hpf	late gastrula 38hpf	late gastrula 65hpf	93hpf	183hpf		
Porites asteroides	Walker et al., 2019	Compared pre-competent and competent planulae						Compared non-probing and probing planulae	
	Mansour et al., 2016	Compared pre-settlement, post-settlement and adult						Calcification, settlement and symbiosis	
Montastrea faveolata	Reyes-Bermudez et al., 2009	Planula, primary polyp and adult						Metamorphosis and onset of calcification	Arrays
Stylophora pistllata	Levy et al., 2021	Planula, primary polyp and adult						Characterisation of single cell types	

***With the exception of those where the methodology is specified, these studies were based on high-throughput sequencing data**